10

X-rays from Cataclysmic Variables

Erik Kuulkers
ESA-ESTEC, SCI-SDG, Keplerlaan 1, 2201 AZ Noordwijk, The Netherlands
& Aurora Technology BV, Hoofdstraat 305, 2171 BG, Sassenheim, The Netherlands

Andrew Norton
Department of Physics & Astronomy, The Open University, Walton Hall, Milton Keynes MK7 6AA, United Kingdom

Axel Schwope
Astrophysikalisches Institut Potsdam, An der Sternwarte 16, 14482 Potsdam, Germany

Brian Warner
Department of Astronomy, University of Cape Town, Rondebosch 7700, South Africa

10.1 Introduction

Cataclysmic Variables (CVs) are a distinct class of interacting binaries, transferring mass from a donor star to a degenerate accretor, a white dwarf (WD). In all observational determinations, and as is required by theory for stable mass transfer, the donor star is of lower mass than the accretor. For comprehensive overviews on the subject of CVs we refer to Hack & La Dous (1993) and Warner (1995).

The majority of CVs have orbital periods, $P_{\rm orb}$, between 75 min and 8 h (see Ritter & Kolb 2003) and consist of Roche lobe-filling main sequence donors and WDs. These are WD analogues of the low-mass X-ray binaries (LMXBs; see §1). In the period range 8 h–3 d the donors must have larger radii than dwarfs in order to fill their Roche lobes and are therefore evolved subgiants. A few CVs are found with $P_{\rm orb}\sim$200 d, which require giant donors for them to be lobe-filling. The absence of evolved CVs with periods ∼3 to ∼200 d is connected with the dynamical instability that results from an initial donor that had a mass larger than about 67% of that of the WD; such binaries will have experienced rapid mass transfer and shortened their periods during a common envelope phase (e.g., Iben & Livio 1993; see also §16). Beyond $P_{\rm orb}\sim$200 d, mass-transferring systems also exist. These constitute the *symbiotic binaries* (SBs) and are in general not Roche lobe-filling, but instead consist of a WD orbiting in the wind of a supergiant, and are thus analogues of the high-mass X-ray binaries (see §1; §5).

At the short end of the period range a different kind of CV exists, i.e., in which the mass losing donors are themselves WDs; they are entirely deficient in hydrogen. These helium-transferring CVs are known, after the type star, as *AM CVn stars* and are observed to have $P_{\rm orb}$ from 60 min down to at least as short as 10 min. They may have evolved by passage through two common-envelope phases, which leaves the cores of both of the component stars exposed (see, e.g, Podsiadlowski et al. 2003, and references therein).

The CVs are divided into subtypes. These were originally based entirely on the behaviour seen in long-term optical light curves, but to this are now added more

subtle parameters such as the presence of polarisation. In essence, a CV's gross behaviour is determined by the rate of mass transfer from the donor, $\dot{M}_{\rm donor}$, and the strength of the magnetic moment, μ, of the WD. Other parameters, such as $P_{\rm orb}$, mass ratio, and chemical abundances, have less effect; but the brightness and spectral variations on an orbital time scale can depend strongly on the inclination.

For $\mu \lesssim 10^{31}\,{\rm G\,cm^{-3}}$ (corresponding to a magnetic field strength $B \lesssim 10^4\,{\rm G}$) the WD is essentially 'non magnetic' (but see §10.5.1) and mass is lost from the donor through a relatively narrow stream onto a so-called accretion disk, from where it spirals inwards until it arrives at the WD (see, e.g., Frank et al. 1992) without any significant magnetic influence on the fluid flow. Even for μ up to $\sim 10^{33.5}\,{\rm G\,cm^{-3}}$ such an accretion stream and accretion disk can form, but the inner regions of the disk are removed by the magnetosphere of the WD, within which fluid flow is magnetically channeled. For larger μ no disk can form at all; the accretion stream from the donor couples onto field lines from the WD before the stream can circle around the WD. These latter two configurations, which apply for typical $\dot{M}_{\rm donor} \sim 10^{-10}$–$10^{-8}\,{\rm M_\odot\,yr^{-1}}$, are known respectively as *intermediate polars* (IPs) for the systems with intermediate field strength, and *polars* (or *AM Her stars*, after the type star) for those with strong fields. The field in polars is so strong that it couples to the field of the donor and forces the WD to corotate with the binary; it also prevents the formation of an accretion disk. In IPs the WD does not corotate. The term *DQ Her star* is often used for IPs of rapid rotation, typically $\lesssim$250 s, but some use the term in place of IP, treating DQ Her as the type star.

Where disks exist there are two principal behaviours, resulting from the different viscosities (and hence ability to transport angular momentum) in cool disks and hot disks (see Lasota 2001; §13). For low $\dot{M}$ through the disk, the disk is lower in temperature and the viscosity is too low to transport mass through the disk as fast as it arrives from the donor; this state is referred to as *quiescence*. The quiescent disk (which is not stationary) therefore acts as a reservoir of gas, and when a critical density is reached it becomes optically thick, heats up and increases in viscosity, and rapidly transfers gas onto the WD. The resultant release of the gravitational energy of the stored gas gives rise to *dwarf nova* (DN) outbursts, during which the optical luminosity is much enhanced. The DN class is subdivided into *U Gem stars* which have outbursts lasting for a few days which recur on time scales of weeks, and *Z Cam stars* where similar outbursts are occasionally interrupted by a standstill at a brightness intermediate between outburst and quiescence. In DN systems with short $P_{\rm orb}$, called *SU UMa stars*, an additional phenomenon occurs – *superoutbursts*, which are typically brighter and last about five times as long as normal outbursts, during which humps in the light curves (so-called 'superhumps') are present with a period of a few % longer than $P_{\rm orb}$. Superoutbursts are thought to be due to tidal stresses between the outer disk and donor, adding to the higher viscous stress in the outer disk; it may even result in additional mass transfer from the donor.

Outbursts, usually of lower amplitude and short duration compared to the DNe, can arise in the truncated disks of IPs. On the other hand, if $\dot{M}_{\rm donor}$ is high enough it can maintain the disk at high viscosity, producing an equilibrium state that does not undergo normal DN outbursts (though modified outbursts are sometimes seen). These systems are known, from the appearance of their spectra, as *nova-like* systems

(NLs). Those showing absorption lines are called *UX UMa stars*, and those showing emission lines are *RW Tri stars*.

The strongly magnetic systems have no disks and therefore lack outbursts. But it is common for polars to show states of low luminosity caused by lowering of $\dot{M}_{\rm donor}$ by as much as two or three orders of magnitude. Other types also show (occasional) low states, especially NLs with $3<P_{\rm orb}({\rm h})<4$, which are known as *VY Scl stars*.

It is supposed that all CVs, with the exception of the helium-transferring AM CVn stars, undergo thermonuclear runaways at the base of the accreted hydrogen-rich layers on the WDs as soon as the layers are massive enough (typically $\sim 10^{-4}\,{\rm M}_\odot$). These produce *classical nova* (CN) eruptions and are in some ways the equivalent of X-ray bursts in LMXBs (see §3). Systems which have shown nova eruptions more than once are referred to as *recurrent novae* (RNe), whereas SBs with nova eruptions are known as *symbiotic novae* (SBNe). Note that some SBNe also recur.

The X-ray behaviours are correlated with the above described optical behaviour of the various CV subtypes, but not always positively. During a DN outburst hard X-rays* have been seen to increase at the beginning (often with a delay of up to a day after the optical outburst begins), but then are suppressed until near the end of the outburst. Similarly, the high $\dot{M}$ (and, therefore, high accretion luminosity) NLs have relatively low X-ray luminosities, $L_{\rm X}$. On the other hand, soft X-ray* fluxes are greatly enhanced during DN outbursts, again with a possible delay with respect to the optical, which is caused by the time taken for an outburst to travel from the cooler outer parts of the disk where it started to the inner disk and the WD/disk boundary layer (BL).

The polars have high soft $L_{\rm X}$ and the IPs have relatively high hard $L_{\rm X}$. All of these different X-ray behaviours are simply connected with the optical depth of the BL in the non-magnetic CVs and with the nature of the channeled accretion flow in the magnetic CVs. More details are given in subsequent sections.

X-rays may also be generated in other parts of CV structures – e.g., in the shock waves where gas ejected by nova eruptions meets the interstellar medium; on the hot WD surface after a nova eruption; and in minor contributions from the magnetically active regions on the surface of the donor.

SS Cyg, one of the optically brightest DNe ($m_{\rm V}\sim$12–8), was the first CV to be detected in X-rays during a rocket flight when it was in outburst (Rappaport et al. 1974). The spectrum was soft with a black-body temperature, $kT_{\rm bb}<130\,{\rm eV}$. In its quiescent state it was first detected by *ANS*, both in soft and hard X-rays. In the soft band, its flux was only a few percent of that observed during outburst (Heise et al. 1978). Since then many more CVs have been detected in X-rays.

We here review X-ray observations of CVs, with some emphasis on what has been achieved in the last decade, up to 2003. For earlier, more general, reviews we refer the interested reader to, e.g., Córdova & Mason (1983), Hack & La Dous (1993), Córdova (1995) and Warner (1995). We note that many CVs have recently been found in globular clusters; we refer to §8 for an overview of this subject.

* With 'soft' and 'hard' X-rays we refer to X-rays with energies of order 10 eV and of order keV, respectively, unless otherwise noted.

10.2 X-ray emission from non-magnetic CVs

10.2.1 General properties

The collective X-ray properties of CVs have been the subject of several studies using observations with *Einstein* (Becker 1981; Córdova & Mason 1983, 1984; Patterson & Raymond 1985a; Eracleous et al. 1991a,b), *ROSAT* (Vrtilek et al. 1994; van Teeseling & Verbunt 1994; Richman 1996; van Teeseling et al. 1996; Verbunt et al. 1997), and *EXOSAT*/ME (Mukai & Shiokawa 1993). For earlier reviews on the X-ray emission from non-magnetic CVs we refer to, e.g., Verbunt (1996) and Mukai (2000). With a few exceptions all non-magnetic CVs radiate at X-ray flux levels $\lesssim 10^{-11}\,\mathrm{erg\,cm^{-2}\,s^{-1}}$ (e.g., Patterson & Raymond 1985a [0.2–4 keV]; Eracleous et al. 1991a [0.1–3.5 keV; 2–10 keV]; Mukai & Shiokawa 1993 [2–10 keV]; Richman 1996 [0.1–2.4 keV]). This translates to, generally, $L_{\rm X} \simeq 10^{29}$–$10^{32}\,\mathrm{erg\,s^{-1}}$. All the CVs below $10^{30}\,\mathrm{erg\,s^{-1}}$ are short-period DNe or low-state magnetic CVs (Verbunt et al. 1997).

Among the non-magnetic CVs the ratio of the X-ray flux to optical and/or UV flux, $F_{\rm X}/F_{\rm opt}$, decreases along the sequence SU UMa stars ($F_{\rm X}/F_{\rm opt} \sim 0.1$) – U Gem stars – Z Cam stars ($F_{\rm X}/F_{\rm opt} \sim 0.01$) – UX UMa stars ($F_{\rm X}/F_{\rm opt} \lesssim 10^{-3}$), due mainly to variations in the optical/UV flux (Verbunt et al. 1997; see also van Teeseling & Verbunt 1994; van Teeseling et al. 1996). There are a few exceptions, however, such as the double degenerate AM CVn systems (§10.2.7). We note that for magnetic CVs $F_{\rm X}/F_{\rm opt}$ is comparable to that of the SU UMa stars (Verbunt et al. 1997). The general pattern is in agreement with Patterson & Raymond (1985a; see also Richman 1996) who find that non-magnetic CVs with high $\dot{M}$ show low $F_{\rm X}/F_{\rm opt}$, and in agreement with the fact that $F_{\rm X}/F_{\rm opt}$ is seen to decrease with increasing $P_{\rm orb}$ (van Teeseling & Verbunt 1994; van Teeseling et al. 1996; see also Córdova & Mason 1984)*. This latter correlation stems from the fact that the UV flux is a strongly increasing function of $P_{\rm orb}$, which in turn is likely related to $\dot{M}$: a high $\dot{M}$ apparently causes the disk to emit more UV flux, but not more X-ray flux (see, e.g., van Teeseling et al. 1996). This general pattern is somewhat perturbed, however, by the anti-correlation between the inclination, i, and the observed X-ray flux (van Teeseling et al. 1996; see also Patterson & Raymond 1985a).

An empirical relation between the equivalent width, EW, of the optical Hβ emission line and $F_{\rm X}/F_{\rm opt}$ exists (Patterson & Raymond 1985a; Richman 1996). This relation predicts $F_{\rm X}/F_{\rm opt}$ to within a factor of 3. The correlation of $F_{\rm X}/F_{\rm opt}$ with EW(Hβ) is thought to also reflect an underlying correlation with $\dot{M}$, since EW(Hβ) is known to correlate with the absolute visual magnitude of the disk, which in turn is correlated with $\dot{M}$ (e.g, Patterson 1984; Warner 1995). Thus low $\dot{M}$ systems produce strong Hβ emission lines and a larger $F_{\rm X}/F_{\rm opt}$.

The absorption column densities, $N_{\rm H}$, as derived from X-ray spectral fits are generally in the range 10^{20}–$10^{21}\,\mathrm{cm^{-2}}$ (e.g., Eracleous et al. 1991a; Richman 1996). VW Hyi has one of the lowest values of $N_{\rm H}$ for any CV ($6\times10^{-17}\,\mathrm{cm^{-2}}$; Polidan et al. 1990), which makes it an ideal CV to study in the EUV and soft X-ray range.

* We caution, however, that the measurements for CVs with short orbital periods are biased towards quiescent systems (i.e., CVs with low $\dot{M}$). X-ray observations of high $\dot{M}$ short orbital period CVs could resolve the issue.

Comparison of the $N_{\rm H}$ values with the colour excess E_{B-V} derived from the 2200Å feature (Verbunt 1987), shows that $N_{\rm H}$ is often higher than predicted on the basis of the average relation derived by Predehl & Schmitt (1995). The excess column may be related to absorbing gas in the CV itself, which can be responsible for some of the orbital variations seen, especially since the CVs displaying highly absorbed spectra are known to have a high inclination (e.g., Eracleous et al. 1991a; Verbunt 1996; see also §§10.2.3, 10.2.4).

The X-ray spectral flux distributions within the 0.5–2.5 keV band seem to be fairly similar for most CVs (Verbunt et al. 1997), although it appears that SU UMa and UX UMa stars have somewhat softer spectra than other DNe and VY Scl stars in their high state (van Teeseling et al. 1996). Individual systems, however, may show significant epoch-to-epoch variability both in luminosity and temperature (e.g., Mukai & Shiokawa 1993). The low signal-to-noise and low resolution X-ray spectra obtained with early X-ray satellites of non-magnetic CVs were generally well described by a bremsstrahlung model (including simple absorption) with typical temperatures in the range 1–5 keV (e.g., Córdova et al. 1981; Córdova & Mason 1983, 1984; Eracleous et al. 1991a; Mukai & Shiokawa 1993). Quiescent DNe are hard X-ray sources with (bremsstrahlung) temperatures of a few keV (e.g., Patterson & Raymond 1985a; Vrtilek et al. 1994) up to ∼10 keV (e.g., Córdova & Mason 1983). However, systematic residuals in the fitted X-ray spectra observed with, e.g., the *Einstein*/IPC and *ROSAT*/PSPC already indicated that the X-ray emission is not well described by the single-temperature models, both for low and high $\dot{M}$ CVs, but instead must be described by a range of temperatures (e.g., Eracleous et al. 1991a; Richman 1996). For more details, see S10.2.5, §10.3.2 and §10.4.4.

If one assumes that the observed X-ray emission comes from a single-temperature model, the emission measure (i.e., the amount of emitting material), EM*, can be determined from the observed photon flux. The EM is not a strong function of $\dot{M}$ (van Teeseling et al. 1996). It decreases, however, for CVs with higher i. For CVs with $i<70°$ this cannot be due to obscuration of the X-ray source by matter in the outer parts of the disk or by the donor. The anti-correlation between EM and i excludes models in which the X-rays are emitted in a relatively large optically thin volume. On the other hand, if the X-rays originate from the inner part of the disk and the scale height of the optically thin X-ray source is not much higher than the disk thickness (as eclipse observations of quiescent DN suggest, see §10.2.3), EM could depend on i. Van Teeseling et al. (1996) come to the conclusion that in high-inclination systems most of the X-ray flux is absorbed by the disk.

So, what is the origin of the X-ray emission in non-magnetic CVs? In the next section we describe the major source of X-rays in these systems, the BL.

10.2.2 The boundary layer model

In non-magnetic CVs the accretion is governed by the disk. Basic theory predicts that half of the gravitational potential energy of the accreting material is liberated through the viscosity in the disk, while the other half is liberated in a boundary layer (BL) between the disk and the surface layer of the WD (e.g.,

* Defined as EM=$\int n_{\rm e}^2 dV$, where $n_{\rm e}$ is the electron density and V the emitting volume.

Shakura & Sunyaev 1973; Lynden-Bell & Pringle 1974; Pringle 1981). Material in the BL moves with Keplerian speeds and collides with the WD which is generally rotating more slowly than break-up velocity. This results in luminosities of the disk and BL of $L_{\rm disk} \simeq L_{\rm BL} \simeq GM_{\rm WD}\dot{M}/2R_{\rm WD}$, where $M_{\rm WD}$ and $R_{\rm WD}$ are the mass and radius of the WD, respectively. For a WD with $M_{\rm WD}=1\,{\rm M}_\odot$, $R_{\rm WD}=10^9\,{\rm cm}$ and $\dot{M}=10^{-10}\,{\rm M}_\odot\,{\rm yr}^{-1}$ this amounts to about $4\times10^{32}\,{\rm erg\,s}^{-1}$. The disk is generally too cool ($kT<1\,{\rm eV}$) to emit X-rays. It radiates mostly at optical and ultraviolet (UV) wavelengths. The BL, on the other hand, mostly radiates in the extreme ultraviolet (EUV) and in X-rays (e.g., Bath et al. 1974b). However, with the modest luminosities the X-rays do not strongly influence the disk, as they do in bright LMXBs.

When $\dot{M}$ is low, such as in DNe in quiescence, the BL is observed to be optically thin. Shocks heat the gas to a temperature of about the virial temperature, $kT_{\rm vir}=GM_{\rm WD}m_{\rm H}/6kR_{\rm WD}\sim20\,{\rm keV}$. When $\dot{M}$ is high, such as in DNe in outburst or in NLs, the BL is observed to be optically thick. Cooling of the BL is efficient and the X-ray spectrum is thermalised with an approximate black-body temperature of $kT_{\rm bb}=(GM_{\rm WD}\dot{M}/8\pi\sigma R_{\rm WD}^3)^{1/4}\sim10\,{\rm eV}$ and $L_{\rm X}>10^{34}\,{\rm erg\,s}^{-1}$ (e.g., Pringle 1977; Pringle & Savonije 1979; Tylenda 1981; Narayan & Popham 1993, Popham & Narayan 1995). The critical $\dot{M}$, $\dot{M}_{\rm crit}$, generally depends on $M_{\rm WD}$ and the viscosity in the disk, and is about $10^{-10}\,{\rm M}_\odot\,{\rm yr}^{-1}$.

Although X-ray observations of CVs are often interpreted within the above described framework of the standard BL model (e.g., many quiescent DNe were found to be modest hard X-ray sources), evidence that BLs really exist in CVs is generally indirect. In the next sections we provide the observational efforts to find this BL, both in quiescence and outburst of DNe, as well as in other high-$\dot{M}$ CVs.

10.2.3 Quiescent dwarf novae

For CVs with $\dot{M}<\dot{M}_{\rm crit}$ Patterson & Raymond (1985a) show that the hard X-ray data from *Einstein* are generally consistent with hot optically thin emission from the BL. The observed temperatures are in the range expected. However, most of these CVs show less BL radiation than predicted (e.g., Pringle et al. 1987; Belloni et al. 1991; van Teeseling & Verbunt 1994; Vrtilek et al. 1994). This also holds for high $\dot{M}$ systems (see §10.2.4), and it is referred to as 'the mystery of the missing BL' (see Ferland et al. 1982). Different explanations for this lack in quiescence have been suggested: disruptions of the inner disk by magnetic fields (Livio & Pringle 1992; Lasota et al. 1995; Warner et al. 1996), coronal siphon flows (Meyer & Meyer-Hofmeister 1994; Lasota et al. 1995), or irradiation by the (relatively) hot WD (King 1997); a rapidly rotating WD (e.g., Ponman et al. 1995); a rapidly spinning accretion belt (Sion et al. 1996); reflection effects and cooling flows (Done & Osborne 1997). Alternatively, the BL largely radiates an additional *very* soft component ($kT\lesssim10\,{\rm eV}$) which would remain undetectable due to interstellar absorption (e.g., Patterson & Raymond 1985b).

High-inclination CVs provide an opportunity to locate the X-ray emitting regions. When the X-ray source is eclipsed one can constrain its size and location using the orbital phase, $\phi_{\rm orb}$, and the duration of ingress and egress. One factor complicating such observations, however, is that eclipsing CVs tend to be fainter in X-rays than

low-inclination CVs, so eclipse studies have been rather count-rate limited (e.g., van Teeseling et al. 1996).

X-ray eclipses have been seen during quiescence of the DNe HT Cas (Mukai et al. 1997; $i \simeq 81°$), Z Cha (van Teeseling 1997a; $i \simeq 82°$) and OY Car (Pratt et al. 1999a; Ramsay et al. 2001a; Wheatley & West 2002; $i \simeq 83°$), as well as during a low state in quiescence of HT Cas (Wood et al. 1995a). They all occur at the time of the optical WD eclipse. The X-ray ingress and egress are rapid; in OY Car their duration is significantly shorter than in the optical (30 ± 3 s vs. 43 ± 2 s; Wheatley & West 2002). This is consistent with the indication that the total X-ray eclipse in HT Cas has a slightly shorter duration than the optical one (by about 27 sec; Mukai et al. 1997). If one assumes that the rapid optical ingress/egress times represent the contact points of the WD with the donor, then the different durations suggest that the X-ray emitting region must be smaller than the WD. The X-rays possibly originate from a broad equatorial belt of which the lower half is absorbed (Mukai et al. 1997; van Teeseling 1997a; Ramsey et al. 2000a; Wheatley & West 2002). This also explains the observed anti-correlation between i and the EM (van Teeseling et al. 1996; see §10.2.1). Since the WD is too cool to produce X-rays, a BL must be responsible for the out-of-eclipse X-ray emission (see Mukai et al. 1997).

In eclipse there is residual X-ray emission at about 1% of the out-of-eclipse flux, with $L_{\rm X} \sim 3 \times 10^{28}\,{\rm erg\,s^{-1}}$ and a soft spectrum ($kT \sim 1$ keV). The fact that this emission in eclipse is softer than that seen out of eclipse seems to rule out the possibility that the residual flux is BL emission scattered into our line of sight by circumstellar material (Wheatley & West 2002). The luminosity (e.g., Rosner et al. 1985; Hempelmann et al. 1995), as well as the temperature (e.g., Schmitt et al. 1990), are consistent with coronal emission from a cool main-sequence donor. Ramsay et al. (2001a), however, argue that the residual emission may come from a weak remnant of a large corona, which is more prominent during outburst (see §10.2.4).

Apart from eclipses, dips in the X-ray light curves have been observed, up to ~50% deep, during quiescence in U Gem (at $\phi_{\rm orb} \sim 0.3$ and 0.8: Szkody et al. 1996, 2000a; $i \sim 65°$), Z Cha ($\phi_{\rm orb} \sim 0.7$–0.8: van Teeseling 1997a), WZ Sge ($\phi_{\rm orb} \sim 0.7$: Patterson et al. 1998; $i \sim 75°$), and OY Car ($\phi_{\rm orb} \sim 0.2$–0.5: Ramsay et al. 2001a). They are only apparent at low X-ray energies, which indicates absorption effects. Similar kinds of dips have also been found during outburst (see §10.2.4).

In order for the dips to be visible at inclinations such as in U Gem the material must be located far from the orbital plane (e.g., Mason et al. 1988; Naylor & La Dous 1997). Note that in quiescence the X-ray dips in U Gem were less deep than during outburst. This means that the X-ray emitting region must be only slightly larger than the outburst BL and that the absorbing material that was present at outburst must maintain a similar location in quiescence. The small residual X-ray flux seen may be scattered into the line of sight from high above the plane (by a disk corona or a wind; e.g., Naylor & La Dous 1997; Mason et al. 1997; see also §10.2.5) or may possibly originate from a hot corona of the donor (Wood et al. 1995b). *HST* observations of OY Car in quiescence show that the UV emission from the WD surroundings is also absorbed by matter above the disk, which is referred to as an 'iron curtain' (see Horne et al. 1994). However, this curtain does not always

seem to exist (Pratt et al. 1999a). Note that no dips were found in the quiescent UV light curves of OY Car (Ramsay et al. 2001a).

Similar kinds of absorption dips have also been seen in IPs (see §10.4), as well as in LMXBs (e.g., Mason 1986; Parmar & White 1988; White et al. 1995; Kuulkers et al. 1998, and references therein; see also §1). Note that column densities of $\lesssim 10^{19}\,\mathrm{cm}^{-2}$ to $\sim 10^{22}\,\mathrm{cm}^{-2}$ in CVs (e.g., Naylor & La Dous 1997) are sufficient to extinguish soft X-ray emission during the dips, whereas maximum column densities of $>10^{23}\,\mathrm{cm}^{-2}$ are typically recorded in LMXBs.

A popular model for the dips is the one outlined by Frank et al. (1987). They explain the dips as the interaction of the accretion stream with the disk, which splashes material out of the plane to form cool clouds that obscure the radiation produced close to the compact object (see also Armitage & Livio 1996, 1998; Kunze et al. 2001). For CVs they predict a single broad dip between phases 0.6 and 0.8, exactly as observed in, e.g., U Gem.

10.2.4 Outbursting dwarf novae and other high-$\dot{M}$ CVs

For most CVs in quiescence $\dot{M}$ onto the WD is of the order of 10^{-12}–$10^{-11}\,\mathrm{M}_\odot\,\mathrm{yr}^{-1}$ (e.g., Patterson 1984; Warner 1995). During an outburst $\dot{M}$ increases by $\sim$2 orders of magnitude, so the disk is likely to cross $\dot{M}_{\rm crit}$. The CV is then expected to change from a hard to a soft X-ray emitter. However, the situation appears to be not that simple, as we will show below.

Soft X-rays have been detected during outbursts of SS Cyg (e.g., Rappaport et al. 1974; Mason et al. 1978; Córdova et al. 1980b; Jones & Watson 1992; Ponman et al. 1995), U Gem (e.g., Córdova et al. 1984), VW Hyi (van der Woerd et al. 1986; Mauche et al. 1991; van Teeseling et al. 1993; Wheatley et al. 1996b), SW UMa (Szkody et al. 1988), and Z Cam (Wheatley et al. 1996a). Other high-$\dot{M}$ CVs generally do not show the soft component (e.g., Silber et al. 1994; van Teeseling et al. 1995). When a soft component is present the X-ray spectra show $kT_{\rm bb}\sim$5–30 eV; these temperatures are similar to the BL temperatures derived from high resolution EUV and X-ray spectra (Mauche et al. 1995: SS Cyg; Long et al. 1996: U Gem; Mauche 1996b: VW Hyi; Mauche & Raymond 2000: OY Car; see also §10.2.5). Note that not all of the soft component is optically thick (Mauche et al. 1995; Long et al. 1996). The soft X-ray fluxes increase by a factor of $\sim$100 from quiescence to outburst. However, they are still too low compared to the simple BL models (e.g., Mauche et al. 1991; van Teeseling et al. 1993; van Teeseling & Verbunt 1994; Ponman et al. 1995; Wheatley et al. 1996b), similar to the discrepancy seen in quiescence (see §10.2.3). A study of the ionisation states inferred from the P Cygni lines arising in winds from high $\dot{M}$ CVs led to a similar conclusion (Drew & Verbunt 1985; Hoare & Drew 1991). Various explanations for the discrepancy (or absence) of soft X-ray flux during outburst have been put forward: differences in $N_{\rm H}$ to different systems (e.g., Patterson & Raymond 1985b; Long et al. 1996); differences in $M_{\rm WD}$ and the WD rotation (see below); absorption in the disk wind (Jensen 1984; Kallman & Jensen 1985); energy loss in the form of a wind (e.g., Silber et al. 1994; Ponman et al. 1995). Moreover, changes in the BL temperature can shift most of the flux out of the soft X-ray bandpass (e.g., Córdova et al. 1980a; Patterson & Raymond 1985b).

Our knowledge of the evolution of the spectral flux distribution during outbursts

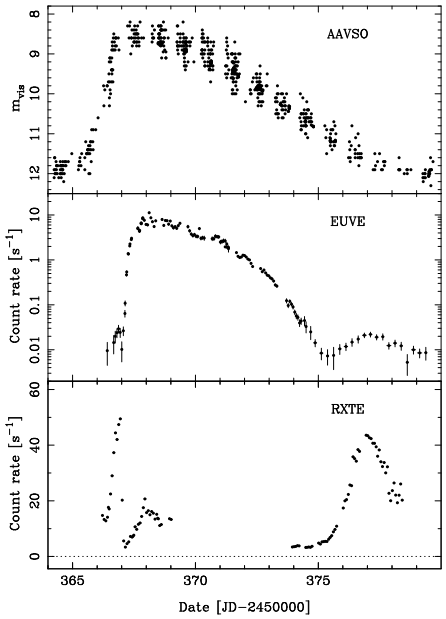

Fig. 10.1. Simultaneous optical (visual and V-band measurements reported to the AAVSO [American Association of Variable Star Observers]), soft X-ray (*EUVE*) and hard X-ray (*RXTE*) observations of SS Cyg throughout outburst. Note that the *RXTE* light curve is plotted on a linear scale in order to emphasize the timing of the sharp transitions. From Wheatley et al. (2003).

of DNe at various wavelengths is mainly based on fragmented (nearly) simultaneous observations. A few dedicated campaigns do exist, however (see, e.g., Pringle et al. 1987; Wheatley et al. 1996b; Szkody 1999, and references therein). One of the most complete coverages to date of a DN outburst is that of SS Cyg (Mauche & Robinson 2001; Wheatley et al. 2000; see Fig. 10.1). We here describe the general behaviour seen at EUV and X-ray wavelengths in outbursting DNe.

The soft X-rays lag the optical outburst light curve by about 12–36 h during the rise (e.g., Jones & Watson 1992; Mauche & Robinson 2001). This is comparable to that measured in the far-UV ($\lesssim$10 eV; Polidan & Holberg 1984). Wheatley et al. (2000) found that the X-ray outburst of SS Cyg started $\sim$18 h *before* the EUV one. The start of the X-ray outburst is marked by a sudden softening of the X-ray spectrum; the rise to soft X-ray maximum is rapid (e.g., Wheatley et al. 2000). After reaching maximum early in the outburst, the soft X-ray flux rapidly decreases again (but less fast than the rise). The decrease is more rapid towards shorter wavelengths. The soft X-rays lead the optical light curve during the decline, and disappear before the end of the optical outburst (e.g., van der Woerd et al. 1986; Mauche & Robinson 2001). The soft X-ray rise and decay times are shorter with respect to the optical (e.g., van der Woerd et al. 1986; Jones & Watson 1992).

The initial soft X-ray rise could be the arrival of the heating wave through the disk at the BL, and the sudden spectral softening is as expected in the BL models. The rapid rise time may represent the time scale of the transition between optically thin and thick emission; the less rapid drop at the end may represent the time scale of the inverse process (e.g., Jones & Watson 1992; Wheatley et al. 2000).

At the time the soft X-rays appear, the hard X-ray flux is suppressed (e.g., Wheatley et al. 2000; Baskill et al. 2001). They do not disappear, however. They stay present during the outburst, with somewhat lower temperature and flux than in qui-

escence. This may be attributed to a density gradient in the optically thick BL, such that there is always a hot optically thin layer which emits hard X-rays (e.g., Patterson & Raymond 1985a; Done & Osborne 1997). The anti-correlation between the soft and hard X-ray flux suggests that we see two physically distinct emission components. The coincidence in the timing show that they are related, however, and possibly mark the time at which the BL becomes optically thick. The hard X-ray flux during outburst is considerably lower than the soft X-ray flux (e.g., ∼0.1% during a superoutburst of VW Hyi; van der Woerd et al. 1986) and it generally declines throughout the outburst (e.g., Verbunt et al. 1999). The temperature of the hard X-ray component increases from outburst to quiescence (e.g., Hartmann et al. 1999). The decline in flux and increase in temperature probably reflects the (slowly) decreasing $\dot{M}$ on the WD (e.g., Jones & Watson 1992; Hartmann et al. 1999).

The hard X-ray flux recovers to quiescent levels just at the very end of the optical outburst (Wheatley et al. 1996b, 2000; see also Yoshida et al. 1992; van Teeseling & Verbunt 1994; Ponman et al. 1995). The recovery time scale is slightly longer than that of the optical decline (e.g., Jones & Watson 1992). The hard X-ray flux varies on a time scale of hundreds of seconds with an amplitude of ∼100% at the start of the recovery to 50% at the end of that observation, with the hardness ratio staying constant. As the end of the optical outburst is thought to correspond to the cooling of the disk region immediately surrounding the WD, this observation indicates that the hard X-rays originate from an area of the disk very close to the WD (e.g., Wheatley et al. 1996b; Verbunt 1996). Note that at the time of the hard X-ray recovery the EUV light curve of SS Cyg exhibited a secondary maximum; this extra emission is consistent with the soft tail of the hard X-ray emission (Mauche & Robinson 2001; Wheatley et al. 2000, 2002).

The situation is different for the outbursts of U Gem, where both soft and hard X-ray fluxes are higher during outburst than in quiescence (by a factor of ∼10–100). The largest increase occurs at EUV wavelengths. This corresponds to the expected increase in an optically thick BL radiating at temperatures near 10 eV at outburst (e.g., Szkody et al. 1999). While the optical flux stays constant near maximum, the EUV flux drops (Long et al. 1996). Assuming the EUV flux originates from near the WD, this suggests that $\dot{M}$ in the innermost regions of the disk decreases compared to the outer regions (which presumably are still optically thick). During the outburst decline, both the soft and hard X-rays decrease faster than the optical flux (Mason et al. 1978; Swank et al. 1978; Córdova & Mason 1984; see also Szkody et al. 1999). Values derived for $L_{\rm BL}/L_{\rm disk}$ are ∼0.5 during quiescence (Szkody et al. 1999), which is among the highest for DNe, and ∼1 during outburst (Long et al. 1996). So, in quiescence, as at outburst, U Gem comes closest to the standard BL model.

There are several reasons why $L_{\rm BL}$ may be larger in U Gem than in systems like VW Hyi (see Long et al. 1996, and references therein). Studies (Pringle 1977; Popham & Narayan 1995) have shown that, when $\dot{M}$ is held fixed, the BL temperature and $L_{\rm BL}$ increase substantially with WD mass. On the other hand, rotation of the WD decreases both the amount of energy released and the effective temperature of the BL. The WD in U Gem is more massive (1.0–1.2 $M_\odot$) than WDs in most DNe and VW Hyi in particular ($\sim 0.6\,M_\odot$). It appears to be at most slowly rotat-

ing ($v \sin i \lesssim 100\,\mathrm{km\,s^{-1}}$), while the WD in VW Hyi rotates with a $v \sin i \simeq 400\,\mathrm{km\,s^{-1}}$ (e.g., Sion et al. 2002), which corresponds to 20% of the break-up velocity.

In contrast to quiescence, there are no eclipses in the X-ray and EUV light curves of OY Car during outburst (Naylor et al. 1988; Pratt et al. 1999b; Mauche & Raymond 2000). The NL UX UMa also does not show X-ray and EUV eclipses (Wood et al. 1995b). This suggests that the prime X-ray source, probably the BL, is obscured at all orbital phases. From contemporaneous observations at other wavelengths (Naylor et al. 1987, 1988), extensive azimuthal structures on the outer disk had been inferred, which may block our view of the BL region. The dips observed in various other CVs (see §10.2.3 and below) are also explained with this geometry. The X-rays we see are thought to be emitted or scattered by a more extended source (e.g., Verbunt 1996); e.g., due to a disk corona (Naylor et al. 1988) or scattering from a photo-ionised disk wind (Raymond & Mauche 1991; Mauche & Raymond 2000; see also §10.2.5).

Dips in the EUV and X-ray light curves during outburst have been seen in U Gem during a normal outburst (at $\phi_{\mathrm{orb}} \sim 0.8$; Long et al. 1996), as well as during an anomalously long ($\sim$45 days) outburst (Mason et al. 1988). As in quiescence (§10.2.3), the dips only occur at low energies, indicating absorption effects. The morphology of the dips changes from cycle to cycle, related to changes in the absorbing material. The dips are deeper at shorter wavelengths, suggesting that the hot central area around the WD is being obscured by cooler material further out. During one dip observed by Mason et al. (1988) the X-ray source was completely extinguished in 15 s, putting the absorbing material near the outer edge of the disk.

10.2.5 X-ray spectral features

As mentioned in §10.2.1, most of the surveys done so far showed that single and sometimes two-temperature bremsstrahlung models were sufficient to describe the CV X-ray spectra, except for the occasional inclusion of a Gaussian to represent a line near 6.7 keV (see below). This is mainly due either to rather poor energy resolution and/or poor statistics. The use of more realistic models was generally not warranted. With the advent of better resolution, larger collecting area, better photon-counting devices, broader band passes, it became clear that the spectra are far more complicated. The X-ray spectra of DNe and NLs can probably be best decribed as somewhere between a pure bremsstrahlung model and a pure coronal model (e.g., van Teeseling & Verbunt 1994). Generally, X-ray spectra from non-magnetic CVs are due to hot thermal plasma in the BL, even at high $\dot{M}$ (e.g., Mukai 2000). This is because the shock-heated plasma in the BL must cool from a temperature near 10 keV indicated by the X-ray spectra to the photospheric temperature of the WD ($\sim$2.5 eV). The situation may be further complicated since X-rays from the hottest gas can photo-ionise cooler gas, altering both the energy balance and the ionisation state at intermediate temperatures.

Many CVs, either in quiescence or in outburst, show an emission line near 6.7 keV from the Kα transition of highly ionised Fe, with EW$\sim$0.8–1.0 (e.g., Szkody et al. 1990); it is associated with the hard X-ray emitting, optically thin plasma. Line emission near 7.9 keV has been reported just after an outburst of SS Cyg (Jones & Watson 1992) and OY Car (Ramsay et al. 2001b). This may be interpreted as thermal Fe-Kβ emission, confirming the origin of line emission from a hot optically

thin region. The presence of an absorption edge near 8.3 keV in the *Ginga* spectrum of SS Cyg implies substantial covering of the hard X-ray emission by the highly ionised gas (possibly a wind). Note that this is hard to reconcile with the picture in which the hard X-rays arise from a hot corona (Yoshida et al. 1992). SS Cyg also shows a reflection component both in quiescence and outburst (Done & Osborne 1997). Its contribution is larger in the softer X-ray spectra seen in outburst than in quiescence. This supports models in which the quiescent inner disk is not present or not optically thick, so that the only reflector is the WD surface rather than the WD plus disk. The amount of reflection in outburst is also more consistent with the hard X-rays forming a corona over the WD surface rather than just an equatorial belt as seen in quiescence. Note that a reflection component is absent in OY Car; this possibly is due to the high inclination, so that it may be obscured by the disk (Ramsay et al. 2001b).

Although observations with the *ASCA* satellite showed complex structures in the X-ray spectra, the spectral resolution was still not high enough to resolve individual lines, especially at wavelengths where many lines are expected (e.g., the Fe L complex around 1 keV). First *EUVE*, and now *Chandra* and *XMM-Newton* carry instruments which provide the opportunity to perform detailed temperature diagnostics from individually resolved lines and line ratios. Line ratios can be used to constrain the electron density, electron temperature, and ionisation balance (see, e.g., Mauche et al. 2001; Szkody et al. 2002a, and references therein). The instruments also provide enough velocity resolution to begin to study the effects of velocity broadening, which gives important clues to whether the emitting region is located in a rapidly rotating BL or is close to the more slowly rotating WD.

High resolution X-ray spectra of U Gem in quiescence (Szkody et al. 2002a) revealed prominent narrow emission lines of O, Ne, Mg, Si, S, and Fe. The line fluxes, ratios, and widths indicate that the X-ray emission lines arise from a range of temperatures in a high density ($>10^{14}\,\mathrm{cm}^{-3}$) gas, moving at low ($<300\,\mathrm{km\,s}^{-1}$) velocity, with a small ($<10^{7}$ cm) scale height compared to the WD radius. This is consistent with the emission coming from an equatorial belt on the WD, as was also inferred from the eclipse light curves (see §10.2.3).

The EUV/soft X-ray spectra of U Gem in outburst ($\phi_{\rm orb}$~0.6–0.8, Long et al. 1996), and OY Car (Mauche & Raymond 2000) and WZ Sge (Kuulkers et al. 2002; Fig. 10.2) in superoutburst resemble each other markedly, and are unlike the spectra seen in other DNe, which is attributed to the high inclination of the former sources. Below ~0.2 keV ($\gtrsim$65Å) they show a 'forest' of broad (FWHM~800–1200 $\mathrm{km\,s}^{-1}$) emission lines of intermediate ionisation stages of N, O, Ne, Mg and Fe, on top of a continuum (which is weak in OY Car and WZ Sge, and appears to be line-free in U Gem). The phase resolved spectra of U Gem show that the eclipses affect the continuum more strongly than the lines, implying that the lines are produced in a region of larger extent than that of the continuum, which is presumably formed in the BL. The line identifications alone significantly constrain the physical nature of the emitting plasma. Because all of the above strong lines are resonance lines, good spectral fits are obtained with a model wherein the radiation from the BL and disk is scattered into the line of sight by the system's photo-ionised disk wind (Mauche & Raymond 2000). Note that the absence of X-ray eclipses in OY Car

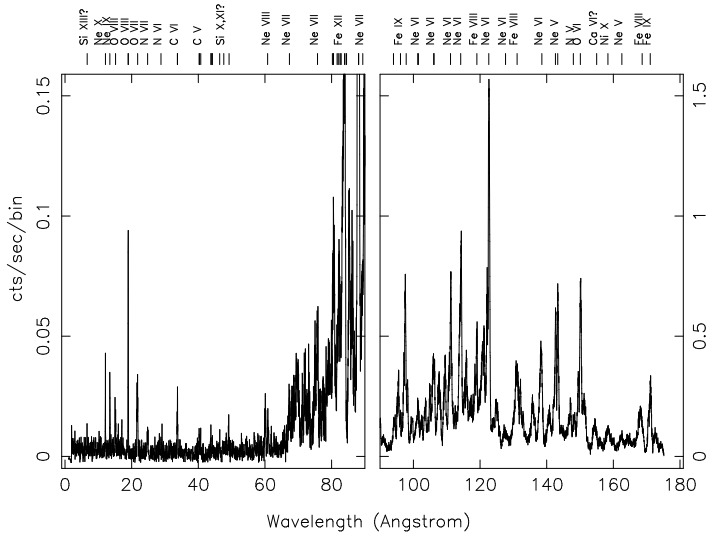

Fig. 10.2. Average Chandra/LETGS spectrum 3.5 d into the superoutburst of WZ Sge. Note the difference in scale between the short and long-wavelength part of the spectrum. Indicated are many of the line identifications. From Kuulkers et al. (2002).

during superoutburst (Naylor et al. 1988) can be understood if much of the X-ray emission we see is light scattered in such an extended wind.

The EUV lines arise from the dominant ionisation states of the wind, and their strengths suggest that the wind mass-loss rate in U Gem is a substantial fraction of the WD accretion rate (Long et al. 1996). The lines are effectively the emission peaks of P Cygni profiles. This requires the scattering region to be of order 10^{10} cm, similar to the size of the region inferred from studies of the UV P Cygni lines in other DNe and NLs. These P Cygni profiles have been shown to arise in strong winds with terminal velocities of order $3000\,\mathrm{km\,s^{-1}}$ (e.g., Drew & Verbunt 1985; Mauche & Raymond 1987; Woods et al. 1990).

WZ Sge's spectrum at higher energies, $\gtrsim$0.2 keV ($\lesssim$65Å), shows weaker lines of highly ionised ions, with O VIII (0.66 keV; 18.9Å) standing out. A strong emission line was also seen near 2.4 keV, probably associated with He-like S XV, which cannot be accounted for using an optically thin thermal plasma model (Kuulkers et al. 2002).

Because of the recent access to high quality X-ray spectra, new interpretations are also emerging. This is demonstrated by, e.g., Mukai et al. (2003), who show that the *Chandra* data of the DNe SS Cyg and U Gem and the old nova V603 Aql are well described by a simple cooling-flow model. This in contrast to three IPs which are better described by a photo-ionisation model.

10.2.6 VY Scl stars

During optical high states the X-ray spectra of NLs can generally be described by emission with temperatures between $kT_{\rm bb}\sim$0.25–0.5 keV and $L_{\rm X}\sim10^{31}$–$10^{32}\,\mathrm{erg\,s^{-1}}$. Since VY Scl stars are thought to have a high $\dot{M}$ during the high state their X-ray spectra are expected to be rather similar to DNe in outburst. However, this seems not to be the case. Distinct differences at other wavelengths exist as well; see Greiner (1999) for an extensive comparison between VY Scl stars and DNe in outburst.

A very soft component ($kT_{\rm bb}\sim19\,$eV) was found in V751 Cyg during an optical low state, at which time the bolometric X-ray luminosity was around 20 times higher ($L_{\rm X}\simeq5\times10^{36}\,{\rm erg\,s^{-1}}$) than in the high state (Greiner et al. 1999; but see Patterson et al. 2001). V Sge showed a similar behaviour: it is a faint hard X-ray source during optical bright states, while during optical low states it shows X-ray luminosities similar to V751 Cyg (Greiner & van Teeseling 1998). $L_{\rm X}$ is clearly higher than generally observed from CVs (see §10.1), and compatible with the lower end of the luminosity distribution of supersoft sources (SSS; see §11). It was therefore suggested that VY Scl stars in their low states may have a link with SSS (Greiner et al. 1999). Not all VY Scl stars in their low state show high values of $L_{\rm X}$, however. Examples are KR Aur with $L_{\rm X}\sim10^{31}\,{\rm erg\,s^{-1}}$ (Eracleous et al. 1991a; Schlegel & Singh 1995) and MV Lyr with $L_{\rm X}\lesssim5\times10^{29}\,{\rm erg\,s^{-1}}$ (Greiner 1999) during a low state.

Moreover, the X-ray spectra during a high (KR Aur) and intermediate (TT Ari) optical state were shown to be poorly described by black-body radiation; a thermal plasma model described the data better. It was concluded, therefore, that the X-ray spectra of VY Scl stars should be interpreted using the latter model, both in the high and low state (Mauche & Mukai 2002). This makes the suggested SSS connection less likely (see also Patterson et al. 2001).

10.2.7 AM CVn stars

The luminosities of the few AM CVn stars that have been detected in X-rays range from $\sim10^{28}$–$5\times10^{30}\,{\rm erg\,s^{-1}}$ (Ulla 1995, and references therein; but see Verbunt et al. 1997). The maximum of the overall flux distribution in AM CVn itself peaks around EUV wavelengths; there is no detectable hard X-ray emission (Ulla 1995). The X-ray luminosities of AM CVn stars agree with the coronal luminosities for single stars (e.g., Rosner et al. 1985; Hempelmann et al. 1995), and possibly with emission from single DB WDs (e.g., Fontaine et al. 1982).

Of the few exceptions to the $F_{\rm X}/F_{\rm opt}$ versus $P_{\rm orb}$ relation (§10.2.1), is AM CVn. With $P_{\rm orb}\sim0.29\,$h it has an unexpectedly small ratio of ~0.002. This small ratio might be explained by a high $\dot{M}$, comparable to UX UMa stars (van Teeseling et al. 1996). On the other hand, the AM CVn system GP Com has a ratio near unity (van Teeseling & Verbunt 1994). This may be due to the fact that the entire disk in GP Com is in a (low) steady state, in which it will always be optically thin, and will not undergo outbursts similar to that seen in DNe (Marsh 1999).

V407 Vul, a CV related to the AM CVn stars, was recently suggested to be a new type of double-degenerate CV (Marsh & Steeghs 2002). In this CV the mass transfer stream may hit a non-magnetic WD directly due to a very compact orbit of 9.5 min. This results in pulsations in the X-ray flux every 9.5 min, with no X-ray emission in between pulses (suggestive for it being a polar [see §10.3], however, neither polarisation nor line emission is seen). Its X-ray spectrum is soft ($kT_{\rm bb}\simeq40$–$55\,$eV; Motch et al. 1996; Wu et al. 2002). This is explained by the stream breaking into dense blobs which are able to penetrate the photosphere of the WD and therefore become thermalised, giving rise to the soft X-ray emission (Marsh & Steeghs 2002).

10.3 X-ray emission from polars

10.3.1 Introduction

In polars, the originally free-falling matter couples to magnetic field lines somewhere between the two stars and is guided to one or two accretion regions in the vicinity of the magnetic poles. These are the sources of intensive X-ray radiation, mainly in the soft X-ray regime, and of cyclotron radiation from IR to UV wavelengths. The observation of pulsed polarised radiation from the cyclotron source led to their nick-names as polars (Krzemiński & Serkowski 1977).

There is no recent review of the X-ray properties of polars in broad generality; the main satellite-related aspects were reviewed (*ROSAT*: Beuermann & Thomas 1993; Beuermann & Burwitz 1995; *EUVE*: Sirk & Howell 1998; Mauche 1999; *ASCA*: Mukai 1995). Emission from post-shock flows in magnetic CVs is described by Cropper (1990).

Just two polars were known as variable stars before the era of X-ray astronomy began (AM Her, VV Pup) and a very small number were detected in optical spectroscopic surveys before 1999 (AN UMa, CE Gru, MR Ser = PG1550+191). To date about 70 polars are known, the vast majority of them identified as counterparts of serendipitous X-ray sources. Only recently, much deeper optical spectroscopic surveys (*Hamburg Schmidt telescope*, *SDSS*) have uncovered new systems in apparently permanent low states of accretion (Reimers & Hagen 1999; Reimers et al. 2000; Szkody et al. 2002b). They were not or just marginally detected in X-rays, and, due to their low accretion rates, display intriguing cyclotron spectra.

Polars are in the first place emitters of soft X-rays. Therefore, the all-sky surveys conducted with *ROSAT* (XRT and WFC) in combination with optical identification programmes permitted for the first time a synoptic view of the CV sky with high sensitivity. Most polars are found below the 2–3 h CV period gap (Webbink & Wickramasinghe 2002). The gap itself is significantly filled in, possibly due to reduced braking by trapping of the wind from the donor within the magnetosphere of the WD (*ibid*). The space density is of the order of $n_s \simeq 1\text{–}2\times10^{-6}\,\mathrm{pc}^{-3}$ of short-period systems and a factor of 10 lower for long-period systems (Beuermann & Schwope 1994).

As shown in Fig. 10.3, polars emit from the IR to the hard X-ray regime. Most of the radiation is accretion-induced. A complete picture therefore requires multi-wavelength observations, preferably obtained contemporaneously because of the inherent high variability on many time scales (from seconds to years). X-ray observations are essential in order to determine the accretion scenarios (which requires one to disentangle the X-ray spectra), the accretion geometries (which requires X-ray observations with full phase coverage), and the accretion history (which requires long-term monitoring in the X-ray domain).

10.3.2 Accretion-induced emission

Matter in the accretion stream is accreted almost vertically on to the magnetic poles of the WD. The accretion process is, therefore, almost always modeled in a one-dimensional quasi-radially symmetric approximation. The presence of, e.g., accretion arcs with corresponding variety of accretion rates and deviations from the

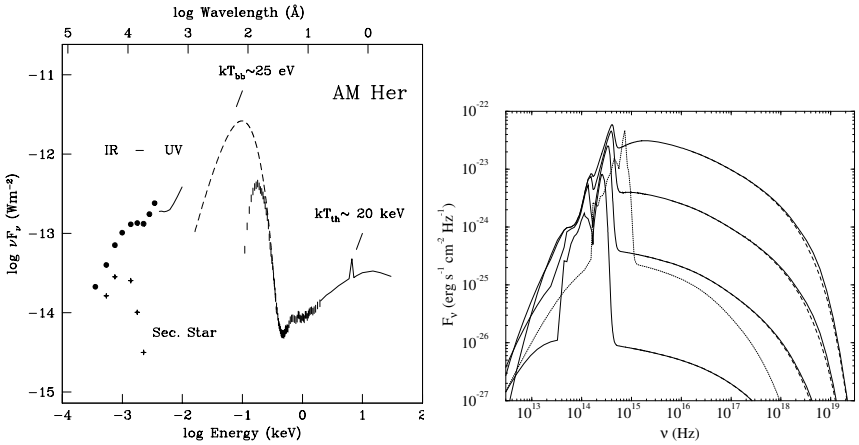

Fig. 10.3. Observed (left, AM Her) and theoretical (right) spectral energy distributions of polars (Beuermann 1999; Fischer & Beuermann 2001). The models do not take into account the prominent soft X-ray component of reprocessed origin, they account for the primary components of optical cyclotron and hard X-ray bremsstrahlung radiation.

radial symmetry due to inclined magnetic field lines is evident from observations but neglected in the modeling for tractability.

Accretion is governed by three parameters, $M_{\rm WD}$, the accretion rate per unit area $\dot{m}$, and B. The balance between those parameters determines whether the acretion region is heated via a strong hydrodynamic stand-off shock or by particle bombardment, and whether the cooling function is dominated by plasma emission or by cyclotron radiation.

With appropriate boundary conditions, the equations of conservation of mass, momentum and energy can be used to calculate the temperature and density as a function of height, as well as the emerging spectra. Only the one-dimensional non-magnetic case could be solved analytically (Aizu 1973). Present numerical models include cooling by cyclotron emission by solving the fully frequency and angle-dependent radiative transfer and treat the accretion plasma in a 2-fluid approximation (Fischer & Beuermann 2001; see Fig. 10.3); they include gravity, account for its variation within the flow and use up-to-date plasma emission codes (Cropper et al. 1998). They take into account pre-shock heating and ionisation, which influences the size of the shock jump and the formation of the emerging spectra. However, current models are still one-dimensional and stationary, which limits their direct applicability to observational data.

Multi-temperature plasma emission models were fitted to the hard X-ray spectra of polars with the aim (among others) to estimate $M_{\rm WD}$. A Compton reflection component from the irradiated WD surface, complex absorption (partial covering cold or warm absorbers) in the pre-shock flow or surrounding matter, fluorescent Kα emission and cold interstellar absorption were taken into account (e.g., Done & Magdziarz 1998; Matt et al. 2000). Such models give satisfactory fits to the data but tend to predict too high values of $M_{\rm WD}$ compared with dynamical mass estimates (Cropper et al. 2000). Van Teeseling et al. (1999) question the validity of coronal models for

the post-shock emission. High $\dot{M}$ systems may be very optically thick in the resonance lines, and the resulting asymmetric line emission may serve as a diagnostic tool to probe the very inner accretion geometry. X-ray line spectroscopy was used to infer sub-solar abundances of the accreted matter (Done & Magdziarz 1998; Ishida & Ezuka 1999), in unresolved conflict with UV-line spectroscopy (Bonnet-Bidaud & Mouchet 1987).

In the 'standard accretion model' (King & Lasota 1979; Lamb & Masters 1979) about half of the X-rays and of the cyclotron radiation are intercepted by the WD surface and are reprocessed as soft X-rays. This simple model predicts about equal luminosities in the bremsstrahlung and cyclotron components on the one hand and the soft emission on the other. Details of this balance depend on the hard X-ray albedo, the irradiation geometry and, observationally, on the viewing geometry. However, since the early days (*EXOSAT* and *Einstein* era), a moderate to strong soft X-ray excess over the other components was observed, creating what was referred to as the 'soft X-ray puzzle'. The size of the soft excess was difficult to assess exactly but X-ray flux ratios $F_{\rm soft}/F_{\rm hard}$ up to $\sim$100 were reported. Difficulties to quantify the soft excess often arise from non-simultaneous observations in the soft and hard spectral bands and from incomplete spectral coverage of the soft component. At temperatures $kT_{\rm bb}\simeq$15–30 eV, it has its peak emission in the EUV, where most instruments have low sensitivity and interstellar absorption is severe. Apart from a few exceptions which indicate the presence of Ne VI absorption edges or Ne VII and Ne VIII absorption lines, the soft spectra can be well described with a simple black body (Mauche 1999). The application of more physical models, e.g., pure-H or solar-abundance stellar atmospheres, does not improve the fits due to the incompleteness of the models and the low signal-to-noise of the data.

Two ways were proposed to solve the soft X-ray puzzle (Kuijpers & Pringle 1982). The first invokes shredding of the stream into diamagnetic blobs in the magnetospheric interaction region. Subsequent confinement and compression of the blobs leads to highly inhomogeneous accretion of filaments with partly or wholly buried shocks (Frank et al. 1988). The primary hard radiation cannot escape freely and the photosphere will be heated from below. Apart from hydrostatic computations of the temperature structure of a one-blob impact (Litchfield & King 1990), this model is not worked out in quantitative detail.

An alternative scenario applies to the low $\dot{m}$ and high B case. In such an environment cyclotron cooling becomes so efficient that it cools the plasma over a mean free path of the infalling particles, i.e., the shock is resolved and bremsstrahlung is suppressed (bombardment solution, Woelk & Beuermann 1996). *ROSAT* observations of a large number of polars showed a clear relation between the size of the soft excess and the magnetic field strength in the accretion region (Beuermann & Schwope 1994; Ramsay et al. 1994)*. This correlation was explained either by enhanced fragmentation of the stream in the magnetosphere, i.e., by enhanced blobby

* Meanwhile, the field strength of about 45 systems have been measured. Some measurements are based on Zeeman-split Balmer-lines from the photosphere or from an accretion halo (Schwope 1996), but most of these measurements are based on the identification of cyclotron harmonic emission lines in low-resolution optical and/or IR spectra, originating from the accretion plasma at one or two accretion regions (for a review see Wickramasinghe & Ferrario 2000).

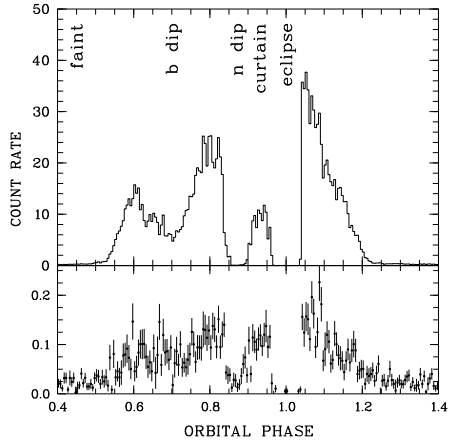

Fig. 10.4. *ROSAT* X-ray light curves of the high-inclination polar HU Aqr. The original photon data comprise 36 ksec and were phase-averaged over the 125 min orbital period. Phase zero corresponds to superior conjunction of the WD. The upper panel encompasses the whole spectral band pass (0.1–2.4 keV), the lower panel only the hard X-ray spectral component (0.5–2.0 keV). Several important features around the orbital cycle are indicated. Adapted from Schwope et al. (2001).

accretion, or by enhanced cyclotron cooling, thus supporting either of the two alternatives to the 'standard' model. The decomposition of light curves in eclipsing systems (e.g., Bailey 1995) and the analysis of soft-to-hard X-ray cross-correlation functions (e.g., Beuermann et al. 1991) suggest that regions with low and high $\dot{m}$ co-exist. Consequently, the accretion region cannot be described in terms of just one of the scenarios. Further modification to the 'standard' model arises from the fact that the reprocessed component in AM Her is observed with the expected energy content but is detected in the UV instead of the soft X-ray regime, suggesting that the soft X-rays are completely decoupled from the other radiation processes (Gänsicke et al. 1995). Similar multi-band investigations including the UV spectral regime are missing for other polars.

10.3.3 X-ray light curves

Polars display a rich phenomenology of X-ray light curves despite their rather simple accretion geometry. The light curves offer large diagnostic potential, since they are modulated by the location and the three-dimensional extent of one or several accretion spots, by stellar eclipses (11 out of 70 systems display stellar eclipses), by non-stationary accretion processes, and by absorption of X-rays within the binary. In the long term the light curves are affected by shifts of the accretion regions in longitudinal and/or lateral directions, by changes between one- and two-pole accretion modes (which gives those systems a completely different appearance) and by large-scale variations of $\dot{M}$. Light-curve changes occur at unpredictable moments and persist for unpredictable duration. It is a common assumption that long-term changes of the accretion rate are related to star spots on the donor at the L_1 (King & Cannizzo 1998) and an attempt has been made to reconstruct a possible pattern of star spots from the accretion history of AM Her (Hessman et al. 2000). While irradiation-induced structure is obvious in Doppler tomograms of the donors, these experiments have failed so far to make star spots visible (Schwope 2001).

The main features of the X-ray light curve of a polar in a one-pole accretion geometry are exemplified in Fig. 10.4, the *ROSAT* light curve of HU Aqr (Schwope et al. 2001). While interpreting these light curves one should bear in mind that the

spin of the WD is synchronously locked with $P_{\rm orb}$, typically to better than 10^{-6} phase units (i.e., $|P_{\rm spin} - P_{\rm orb}|/P_{\rm orb} < 10^{-6}$). This implies that any phase information can be easily transformed to angular information, either in the frame of the WD or in the frame of the binary star, provided the phase of conjunction of the WD is known. The light curve shows a pronounced bright-faint pattern, with the bright phase lasting from phase 0.53 to 1.22 (Fig. 10.4). Further features modulating the bright phase are labeled broad dip ('b dip'), narrow dip ('n dip'), curtain, eclipse, and are discussed below. The faint phase is caused by a so-called self-eclipse of the accretion region by the WD. In the faint phase some residual X-ray emission is present, which is probably of scattering origin. The length and phasing of the bright phase allows clues to be drawn on the latitude and longitude of the accretion spot. Most polars have the main accretion spot in the quadrant of the ballistic stream (seen by a hypothetical observer on the WD), i.e., on the leading side of the WD. However, a few systems have their spots on the trailing side of the WD or even on the opposite side from the donor. This implies complex motions of matter in the magnetosphere and it is by no means clear to what extent the simple picture of accretion via Roche-lobe overflow at L_1 is applicable. Recent Doppler tomograms show that even the putative ballistic, freely falling stream in the vicinity of the L_1 might be influenced by the magnetic fields in the binary (Schwarz et al. 2002). The spots do not show any preferred latitude, i.e., the spin axis of the WD seems not to be aligned with the rotation axis.

While the hard X-rays are assumed to be formed by (mainly) optically thin plasma radiation, the X-ray brightness should be constant throughout the bright phase. Instead, large fluctuations are seen which are assigned to non-stationary accretion and occultations. The soft X-rays originate from optically thick surfaces and orbital modulations are expected (and observed) to be more marked. The bright phase in general is far from being compatible with a flat accretion spot and heating by accretion blobs rather than irradiation plays an important role. The depth-dependent temperature structure in the vicinity of an accretion filament was computed by Litchfield & King (1990) using similarity to a heat conduction problem. The photosphere is then assumed to be shaped like a mound, but its height proved not to be sufficient to reproduce soft X-ray light curves of, e.g., the anomalous state of AM Her (Heise et al. 1985), suggesting that hydrodynamic splashes rather than a hydrostatic atmosphere are responsible for the soft X-ray light curves.

The bright phase may undergo shifts with respect to binary phase zero. In some cases this reflects the accretion rate dependent penetration of the magnetosphere by the ballistic stream before it gets threaded onto magnetic field lines. In other cases it indicates a small asynchronism of $P_{\rm spin}$ and $P_{\rm orb}$ (Schwope et al. 2001, 2002).

There are 11 eclipsing systems; two of them, UZ For and HU Aqr, were found bright enough to resolve the ingress into or the egress from the eclipse in soft X-rays. Detailed modeling shows that the soft X-ray accretion spots have an angular lateral extent of less than 5° (Warren et al. 1995; Schwope et al. 2001) and a vertical extent of less than $0.05\,{\rm R_{WD}}$. Hence the soft X-ray accretion region is pillbox-shaped rather than pencil-shaped.

The narrow dip is due to absorption in the accretion stream, which has coupled to the magnetic field and has left the orbital plane. This material may intercept X-rays from the accretion hot spot at certain phases. Those features can be observed only in

systems where the accretion stream (or curtain) and the observer are located in the same hemisphere with respect to the orbital plane. Furthermore, the orbital inclination must be sufficiently high and the inclination of the magnetic axis sufficiently low. This ensures the the stream is raised sufficiently high above the plane and the line of sight to the accretion spot crosses the accretion stream. The orbital phase of this feature indicates the azimuth and its width the size of the threading region in the magnetosphere. To a first order, the coupling region is located where the magnetic pressure overcomes the ram pressure of the ballistic stream. A simultaneous hard X-ray and near-IR study of the dips in EF Eri (Watson et al. 1989) demonstrates the presence of substantial structure in the dips, implying significant density fluctuations in the stream, either spatial or temporal. The origin of the broad dip centred at an earlier phase remains unclear so far. Its width and X-ray colour suggest an origin in warm absorbing matter in close vicinity to the hot accretion spot. Its diagnostic potential needs to be explored.

10.4 X-ray emission from intermediate polars

10.4.1 Introduction

The first of the asynchronous magnetic CVs to be discovered was the remnant of Nova Herculis 1934 – DQ Her – in 1954. Walker (1956) found a highly stable 71.1 s optical modulation with an amplitude of a few hundredths of a magnitude, which disappeared during eclipse. In analogy with the models for X-ray pulsars (Pringle & Rees 1972; see §7) an accreting oblique dipole rotator was eventually suggested (Bath et al. 1974a). The correctness of this model was demonstrated by the discovery of a phase shift in the 71 s signal during eclipse that could be matched to the eclipse of a beam of high energy radiation, emitted by the rotating WD, as it swept over the accretion disk and was reprocessed into optical wavelengths (Warner et al. 1972; Patterson et al. 1978).

The evident success of this accreting magnetic model led to its adoption when the first X-ray CVs to have two simultaneous periodic modulations were found. For example, AO Psc was observed to have a strong 14.3 min optical periodicity (Warner 1980; Patterson & Price 1980) but a 13.4 min modulation in hard X-rays (White & Marshall 1980). The realisation that the frequency difference of these two modulations is equal to the orbital frequency showed that the X-ray period arises from rotation of the WD, but the optical modulation must be caused by the rotating beam being reprocessed from some structure fixed in the rotating frame of the binary (e.g., the donor or the thickening of the disk where the stream impacts). It was therefore recognized that only two 'clocks' are really present, i.e., $P_{\rm orb}$ and the spin period of the WD, $P_{\rm spin}$.

Because of amplitude modulation, caused largely by geometrical projection effects, a suite of modulations is sometimes seen in optical observations. Denoting $\Omega{=}2\pi/P_{\rm orb}$ and $\omega{=}2\pi/P_{\rm spin}$, the frequencies $\omega{-}\Omega$, $\omega{-}2\Omega$, $\omega{+}\Omega$ and $\omega+2\Omega$ are predicted to occur (Warner 1986). The importance of these sidebands is that they act as proxies for X-rays in those cases where no X-ray modulation has been observed; there are no models other than IPs* that explain the presence of orbital sidebands.

* The name 'intermediate polar' was introduced by Warner (1983).

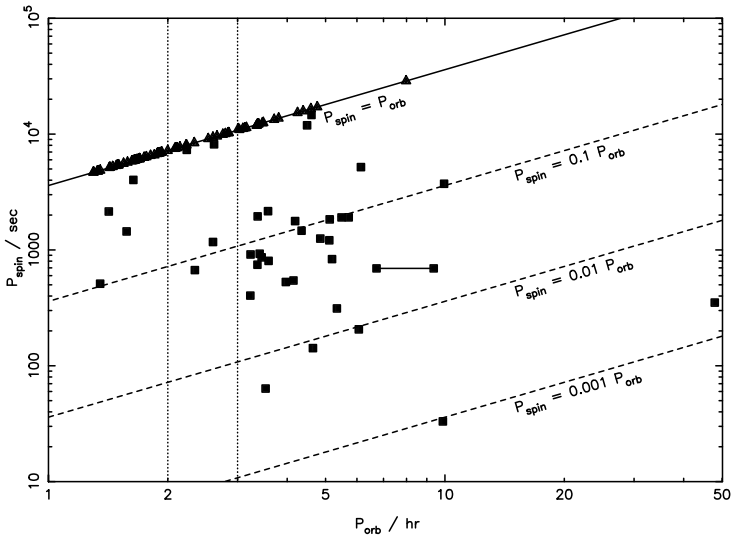

Fig. 10.5. The $P_{\rm spin}$ versus $P_{\rm orb}$ diagram of magnetic CVs. Polars are indicated by triangles; IPs are indicated by squares. From Norton et al. (2004).

Direct observation of an X-ray modulation, usually denoting $P_{\rm spin}$, accompanied by $P_{\rm orb}$, usually obtained from optical photometric or spectroscopic observations, is required to give full conviction to classification as an IP. But an optical periodicity of proven stability (to distinguish from the quasi-periodic oscillations discussed in §10.5), and the presence of one or more orbital sidebands, even without any X-ray detection at all, give an irresistible urge for inclusion in the IP lists. The parameter space occupied by the IPs is illustrated in Fig. 10.5.

10.4.2 Modes of accretion

Most IPs are expected to accrete via some form of truncated accretion disk whose inner edge is at the magnetospheric radius. From here, material will attach onto field lines and flow towards the magnetic poles, forming 'accretion curtains' above each pole (Rosen et al. 1988). Unlike the polars, the accretion flow impacting the WD in IPs will therefore be more extended, occurring over a greater fraction of the WD surface. At some point in the flow, the material will experience a strong shock before settling and cooling mainly by thermal bremsstrahlung. This region is thus the origin of the observed X-ray emission. Modulation at the WD spin period is produced by a combination of self occultation and varying photo-electric absorption towards the X-ray emission sites.

Some IPs are also believed to accrete (at least in part) directly via a stream, in a similar manner to polars. This stream may overflow a disk (disk-overflow accretion; e.g., Hellier et al. 1989; King & Lasota 1991; Armitage & Livio 1996) or replace a disk entirely (stream-fed accretion; Hameury et al. 1986). As the stream flips from pole to pole, this will naturally give rise to an X-ray modulation at the sideband frequency $\omega-\Omega$ (Hellier 1991; Wynn & King 1992; Norton 1993). In disk-fed accretion it is likely that the footprints of the field lines onto which the flow attaches are semi-

circular X-ray emitting arcs around each magnetic pole, and are fixed on the surface of the WD. By contrast, the field lines to which the stream-fed or disk-overflow accretion attaches are likely to have smaller footprints at each magnetic pole and these will 'migrate' around the pole to follow the incoming stream, as a function of the sideband phase (Norton et al. 1997).

10.4.3 X-ray light curves

In early X-ray observations, the light curves of IPs folded at the WD spin period were seen to be roughly sinusoidal and interpreted as largely due to self occultation of the emission area by the WD (King & Shaviv 1984). First hints that this was not the case came with *EXOSAT* observations (Mason 1985; Watson 1986; Norton & Watson 1989) which showed that the modulation depth tended to increase with increasing X-ray energy over the range 1–10 keV, indicating that photo-electric absorption made some contribution to the observed modulation.

The now widely accepted 'accretion curtain' model was proposed to explain the data from EX Hya (Rosen et al. 1988, 1991). In this model, the emission region is a tall, thin, arc-shaped curtain and the largest X-ray flux is seen when the curtains are viewed from the side (i.e., when a given pole is pointing *away* from the observer). Although EX Hya is an atypical IP, such a model was also successfully applied to the other IPs (e.g., Hellier et al. 1991).

Ginga, *ROSAT*, *ASCA* and *RXTE* each observed many IPs, producing light curves with extremely high signal-to-noise in many cases. Whilst the pulse profiles of some sources (e.g., EX Hya; Rosen et al. 1991) still appear roughly sinusoidal, there are indications that additional structure may be present in others. For example, the combined *ROSAT* and *Ginga* pulse profiles of AO Psc and V1223 Sgr show evidence for a small notch superimposed on the peak of the pulse (Taylor et al. 1997). Several objects, including GK Per (Ishida et al. 1992), XY Ari (Kamata & Koyama 1993), V405 Aur (Allan et al. 1996), YY Dra and V709 Cas (Norton et al. 1999) show pulse profiles that are double peaked (at least on some occasions). Some of the most complex pulse profiles are those seen from FO Aqr (Norton et al. 1992a; see Fig. 10.6), BG CMi (Norton et al. 1992b) and PQ Gem (Duck et al. 1994) which show narrow notches superimposed on broader modulations and pulse profiles that change significantly with $\phi_{\rm orb}$. Many of these X-ray pulse profiles also vary dramatically on time scales of months or years. For instance, those of GK Per and XY Ari are single peaked in outburst (Watson et al. 1985; Hellier et al. 1997) but double peaked in quiescence; in other cases, such as V709 Cas, the contributions of various harmonics of the spin frequency are seen to vary (de Martino et al. 2001).

It has been noted (e.g., Norton et al. 1999) that the IPs exhibiting double-peaked X-ray pulse profiles are mostly those with short $P_{\rm spin}$. The WDs in these objects therefore probably have weak magnetic fields, so the magnetospheric radius is relatively small. Consequently the footprints of the disk-fed accretion curtains on the WD surface are relatively large. In contrast to a conventional accretion curtain, the optical depths to X-ray emission are therefore lowest in the direction along the magnetic field lines, and highest in the direction parallel to the WD surface, such that the emission from the two poles conspires to produce double-peaked X-ray pulse profiles (Allan et al. 1996; Hellier 1996; Norton et al. 1999). Such a pulse profile is therefore

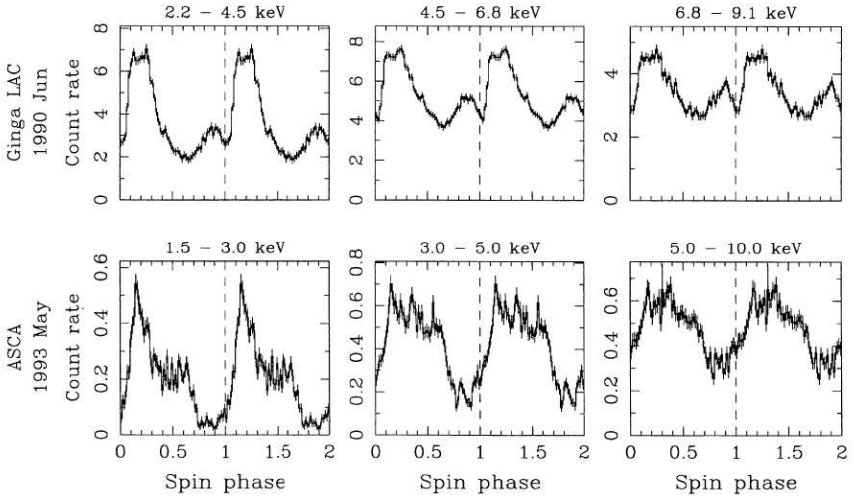

Fig. 10.6. X-ray pulse profiles of FO Aqr. Adapted from Beardmore et al. (1998).

not a unique indicator of two-pole accretion. Indeed, two-pole accretion onto smaller regions of the WD surface may be considered the 'normal' mode of behaviour in a disk-fed IP with a longer $P_{\rm spin}$ (and therefore a higher field strength), resulting in a single-peaked pulse profile. Indications of the size of the X-ray emitting region in IPs have come from a study of the deeply eclipsing IP XY Ari. The $\lesssim$2 s egress from eclipse seen in *RXTE* data limits the accretion region to $\lesssim$0.002 of the WD surface area (Hellier 1997).

Whereas fast rotators with relatively weak fields show double-peaked pulse profiles, several slower rotators with larger fields (and therefore larger magnetospheres) have been seen to exhibit an X-ray sideband modulation (i.e., at a frequency $\omega-\Omega$) at some time. A strong sideband signal is seen in TX Col (Buckley & Tuohy 1989), and FO Aqr (Norton et al. 1992a), and weaker signals in AO Psc and V1223 Sgr (Hellier 1992). A dominant sideband period may exist in BG CMi (Norton et al. 1992b). Observations of V2400 Oph subsequently confirmed this system as the first truly diskless IP by revealing that its X-ray signal varies *only* at the 1003 s sideband period (Buckley et al. 1997; Hellier & Beardmore 2002).

The relative strengths of the X-ray sideband and spin modulation in FO Aqr have been seen to vary on time scales of years (Beardmore et al. 1998) and those in TX Col on time scales as short as months (Norton et al. 1997). The interpretation is that the relative amounts of accretion occurring via a stream and via a disk vary, possibly due to changes in $\dot{M}$ or other activity on the donor near to the L_1 point.

IPs sometimes show strong orbital modulations in their X-ray light curves. The compilation by Hellier et al. (1993) showed that FO Aqr, EX Hya, BG CMi and AO Psc all have orbital dips characterized by increased photo-electric absorption around $\phi_{\rm orb}\sim$0.8. Such orbital modulations have been confirmed by subsequent observations (e.g., Norton et al. 1992a,b; Taylor et al. 1997; Allan et al. 1998). Hellier

et al. (1993) concluded that the cause was likely to be similar to that in DNe and LMXBs and due to material thrown out of the orbital plane by the stream impact with the disk or the magnetosphere (see §10.2.3). Alternatively, or additionally, a spin pulse profile that varies with $\phi_{\rm orb}$ (such as will arise naturally in a stream-fed or disk-overflow model) will naturally give rise to an orbital modulation. It is likely that this effect contributes to the observed orbital modulation, at least in some systems.

10.4.4 X-ray spectra

The relatively low signal-to-noise and low resolution X-ray spectra of IPs obtained with *EXOSAT* were adequately fitted with single temperature (∼10's of keV) bremsstrahlung continua (see §10.2.5) passing through a partial absorber which varied with phase (see the compilation by Norton & Watson 1989). Fluorescent Fe Kα lines were also seen in most IPs (Norton et al. 1991). *Ginga* observations largely confirmed these results but showed that both thermal and fluorescent contributions to the Fe lines were present (Ishida 1991). The higher spectral resolution of *ASCA* allowed more emission lines to be detected in the X-ray spectra of EX Hya (Ishida & Fujimoto 1995) and AO Psc (Fujimoto & Ishida 1995; Hellier et al. 1996), for example, and also showed that V405 Aur, PQ Gem, AO Psc, BG CMi, V2400 Oph, TV Col and V1025 Cen have thermal Fe Kα lines that are broadened by ∼200 eV (Hellier et al. 1998). In each case, up to three Gaussian lines were required, corresponding to cold, H-like and He-like Fe.

A significant advance in the modelling of IP X-ray spectra came with models that used a multi-temperature emission region, including effects such as reflection from the surface of the WD and partially ionised absorbers (e.g., Cropper et al. 1998; Beardmore et al. 2000). Using this technique, Cropper et al. (1998) fitted the *Ginga* spectra of 9 IPs and determined WD masses for them.

ROSAT discovered a sub-class of IPs, e.g., V405 Aur, PQ Gem and UU Col, characterized by soft X-ray spectra, with black-body components at $T_{\rm bb}$ of ∼10's of eV (Mason et al. 1992; Haberl et al. 1994; Haberl & Motch 1995; Burwitz et al. 1996). The soft X-rays from these objects probably originate, as in polars, from the heated WD surface around the accreting poles. The black-body fluxes indicate fractional areas of only $\sim 10^{-5}$ of the WD surface for the soft X-ray emission region (Haberl & Motch 1995).

At the time of writing, *Chandra* and *XMM-Newton* spectra of IPs are just becoming available and will probably revolutionize our understanding of IP X-ray spectra. For example, Mauche (2002b) shows that line ratios from the *Chandra* spectrum of EX Hya may be used to determine a plasma temperature which spans the range 0.5 to 10 keV and a plasma density $n \gtrsim 2 \times 10^{14}$ cm^{-3}. Mukai et al. (2003) demonstrate that EX Hya's *Chandra* spectrum is well fit by a simple cooling-flow model, as are those of the DNe U Gem and SS Cyg, and the old nova V603 Aql. In contrast, the *Chandra* spectra of the IPs V1223 Sgr, AO Psc and GK Per are inconsistent with such a model, but conform with the expectations for line emission from a photo-ionised plasma.

10.5 Rapid oscillations

10.5.1 Dwarf nova oscillations

10.5.1.1 Introduction

The rapid oscillations seen in DQ Her (at 71.1 s, see §10.4.1) and AE Aqr are of very high stability ($|\dot{P}|^{-1}>10^{12}$). In contrast, optical oscillations of low stability ($|\dot{P}|^{-1}\sim10^{4-6}$) were discovered in some high $\dot{M}$ CVs (namely, DNe in outburst and NLs) by Warner & Robinson (1972). These are known as dwarf nova oscillations (DNOs) and are usually of very low amplitude (typically less than 0.01 mag) and span the range 5–100 s, with a concentration near 25 s. In a given CV they always appear at similar periods. Their short periods indicate a source near to the WD, and there was early expectation that they would be found at short wavelengths. They were indeed later found in the soft X-ray, EUV and UV regions. Only recently, however, have simultaneous EUV and optical observations of DNOs shown that, again as expected, the same phenomenon is being observed in all wavelength regions (Mauche & Robinson 2001) – but frequently the optical modulated flux is merely reprocessed X-ray and EUV radiation.

Before discussing observations of X-ray DNOs we describe a physical model that is gaining acceptance as an explanation of the DNOs. In its essence it is an IP model, but the magnetic field lines are connected to the accreted material near the equator of the WD, and not rooted in its interior. Paczyński (1978) pointed out that if the intrinsic field of the WD is low enough ($B\lesssim10^5$ G: Katz 1975) the accreted material will be able to circulate around the equator of the WD. (The high Q of DQ Her shows that in that CV the field is strong enough to lock the exterior layers to the interior, so the accretion torque is applied to the entire WD.) The shear in the accreting equatorial belt may generate a field strong enough to control the gas flow near the surface of the WD – but $P_{\rm spin}$ of the belt is determined by magnetic coupling to the inner edge of the disk. As $\dot{M}$ waxes and wanes during a DN outburst the inner radius (and Keplerian period) of the disk is first reduced and then increased. The result is a low inertia magnetic accretor (Warner & Woudt 2002), which explains the large range of a DNO period during a DN outburst, and why it is observed to reach a minimum value at the maximum of $\dot{M}$. There is direct spectroscopic evidence for rapidly spinning equatorial belts in DNe during outburst (e.g., Sion et al. 1996).

10.5.1.2 Soft X-ray DNOs

Our knowledge of the oscillations in soft X-rays (0.1–0.5 keV) during outbursts of DNe is dominated by observations made of SS Cyg, U Gem and VW Hyi; all relatively nearby and optically bright objects. The first detections were in SS Cyg (Córdova et al. 1980b, 1984), U Gem (Córdova et al. 1984) and VW Hyi (van der Woerd et al. 1987). Modulated soft X-ray emission appears in all of the observed SS Cyg outbursts, but in only one of three observed U Gem outbursts. The hard X-ray emission in SS Cyg is not modulated (Swank 1979). The soft X-ray modulation amplitudes are much greater than in the optical; generally $\sim$25%, but as much as 100% for individual cycles. This shows that much of the accretion luminosity is involved in the modulation process. Other DNOs have been detected, i.e., in the DN HT Cas and the NLs YZ Cnc, RW Sex and AB Dra (Córdova and Mason 1984),

Table 10.1. *EUV and Soft X-ray DNOs in DNe during outburst.*

Star	$P_{\rm orb}$ (h)	Period (s)	References
SS Cyg	6.60	9	Córdova et al. (1980b)
		10.7	Córdova et al. (1984)
		9.6–10.1	Watson et al. (1985)
		7.4–10.4	Jones & Watson (1992)
		7.2–9.3	Mauche (1996a)
		2.8*	van Teeseling (1997b)
		2.9–8.2	Mauche & Robinson (2001)
		9.1	Mauche (2002a)
U Gem	4.25	25–29	Córdova et al. (1984)
		∼25	Long et al. (1996)
VW Hyi	1.78	14.06–14.4	van der Woerd et al. (1987)

*A frequency doubling had occurred.

but the last three are more probably of the quasi-periodic type discussed in §10.5.2. Table 10.1 lists the published studies of the three bright DNe.

The SS Cyg observations by Córdova et al. (1980b, 1984) provided the first means of analysing the short-term temporal variations of the DNOs; in the X-ray region individual cycles can be seen, whereas in optical observations the DNOs are only seen in Fourier transforms (FTs). However, later observations of rare large amplitude optical DNOs, especially those in the DN TY PsA (Warner et al. 1989), showed behaviour similar to that in X-rays, namely that the DNOs maintain relatively high coherence for a time ΔT and then jump suddenly (t<100 s) to a period typically 0.02 s different. These jumps in period can be in either direction and are superimposed on the steady increase or decrease in period associated with, respectively, decreasing or increasing luminosity. When the luminosity is not changing rapidly, i.e., in NLs or in DNe near maximum light, ΔT can be in excess of an hour; but late in an outburst ΔT decreases to hundreds of seconds and the DNOs become incoherent and difficult or impossible to detect with FT techniques.

In the past five years considerable progress has been made in two areas: the observation of DNOs in the EUV flux (which may be assumed to be a proxy for X-ray modulation) and the extension of studies in the optical. Mauche (1996a, 1997) and Mauche & Robinson (2001) have studied the EUV during outbursts of SS Cyg and discovered several new phenomena, including a frequency doubling of DNOs near maximum of outburst. This shows as a reduction of DNO period from ∼6 s to ∼3 s; X-ray observations made near maximum of a different outburst of SS Cyg also showed the ∼3 s modulation (van Teeseling 1997b). It is possible that the effect is in essence geometrical, with emission from two accretion poles being seen when the inner edge of the disk is very close to the WD surface (Warner & Woudt 2002).

Optical studies of VW Hyi (Woudt & Warner 2002; Warner & Woudt 2002) show the correlation of DNO period with luminosity, detecting for the first time oscillations at ∼14 s near maximum, which were previously only seen in X-rays (van der Woerd et al. 1987). A rapid slowdown of the DNOs, from a period ∼20 s to ∼40 s over about

6 h, coincides with the epoch when the EUV flux plummets almost to zero, and is interpreted as a propeller phase in which accretion is prevented by the magnetic field attached to the rapidly spinning equatorial belt. Following the propeller phase a frequency doubling occurs, which may be a change (at least in visibility) from single pole to two-pole accretion.

X-ray modulations at 27.87 s in WZ Sge in quiescence (Patterson et al. 1998) supports the magnetic accretion model for their origin (see, e.g., Warner & Woudt 2002, and references therein). Their behaviour in the UV during superoutburst (Knigge et al. 2002), for example the lack of coherence and the occurrence of harmonics, also resembles DNO behaviour.

10.5.2 Quasi-Periodic Oscillations

In 1977 a second class of unstable optical oscillations was found during dwarf nova outbursts; these have $Q \sim 5$, which means that (as they are spread over a wide range of frequency) they are hard to detect in FTs and were only noticed because of large amplitude in the light curve (Patterson et al. 1977). Their low coherence gives them the name 'quasi-periodic oscillations' (QPOs). They have time scales typically an order of magnitude longer than the DNOs, can be present or absent during outbursts, and are independent of whether DNOs are active. They have been commonly seen in DN outbursts and in NLs, and even occasionally in DNe at quiescence (Warner 1995; Woudt & Warner 2002).

Very few observations of CV QPOs in X-rays have been made. In soft X-rays a very low amplitude signal at 83 s in SS Cyg during one outburst was found, and 111 s in another (Mauche 1997, 2002a); Córdova & Mason (1984) found a 12% amplitude modulation at 585 s in U Gem during outburst and Ramsay et al. (2001a) found a modulation at 2240 s at low energies in OY Car just after the end of an outburst. At higher energies (2–10 keV) large amplitude ~500 s modulations in VW Hyi in the final stages of decline from an outburst were found (Wheatley et al. 1996b).

A third class of optical oscillations has recently been recognized (Warner et al. 2003), which are present during outburst and even very occasionally in quiescence, and change very little in period throughout the outburst of a DN. They are represented by the ~88 s oscillations in VW Hyi (Haefner et al. 1979), the ~33 s oscillations in SS Cyg (Patterson 1981) and the ~92 s oscillations in the NL EC 2117−54 (Warner et al. 2003). They are typically a factor ~4 longer in period than the standard DNOs. They may be represented in X-rays by the ~130 s periodicities seen in U Gem during outburst (Córdova et al. 1984; Córdova & Mason 1984).

¿From the rich phenomenology of optical DNOs and QPOs in dwarf nova outbursts (especially VW Hyi) it has been suggested that the QPOs are caused by slow progradely travelling waves in the inner disk; probably close to the inner radius where magnetic channelling begins (Warner & Woudt 2002). Then the optical QPOs are caused by 'reflection' and obscuration of radiation from the central regions of the disk and WD.

In the X-ray region quasi-periodic obscuration would account for the modulations listed above. In all of those cases the X-ray QPOs are similar in time scale to the optical QPOs in the same stars; no simultaneous observations in optical and X-rays have yet been made. The newly recognized longer period DNOs probably arise from

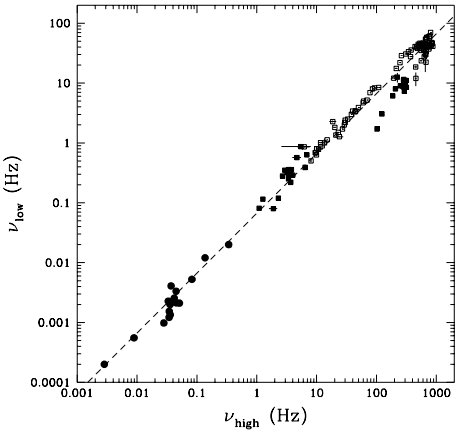

Fig. 10.7. The 'two-QPO diagram' for LMXBs (filled squares: black hole binaries; open squares: neutron star binaries) and 17 CVs (filled circles). The LMXB data are from Belloni et al. (2002). The dashed line marks $P_{\rm QPO}/P_{\rm DNO}$=15. ¿From Warner et al. (2003).

magnetically controlled accretion onto the body of the WD itself (rather than just its equatorial belt).

10.5.3 The CV Two-QPO Diagram

The optical DNOs and QPOs in CVs behave in a fashion similar to what is seen in the high and low frequency QPOs in LMXBs (Psaltis et al. 1999; §2.7), namely that $P_{\rm QPO}{\sim}15P_{\rm DNO}$ (Warner & Woudt 2002; Mauche 2002a; Fig. 10.7). The X-ray DNOs and QPOs in SS Cyg agree with this relationship (Mauche 2002a), and the optical modulations in VW Hyi follow such a relationship over a range of a factor of two as the star decreases in brightness at the end of outburst (Woudt & Warner 2002). Furthermore, the CV 'two-QPO diagram' (i.e., treating the DNOs as higher frequency QPOs) is an extension of that in X-rays to frequencies three orders of magnitude lower (Warner & Woudt 2002; Warner et al. 2003; Fig. 10.7).

10.6 X-ray emission from novae

For earlier X-ray reviews of novae we refer the interested reader to, e.g., Ögelman & Orio (1995), Orio (1999), and Krautter (2002).

10.6.1 X-ray emission mechanisms

In novae, after the thermo-nuclear runaway in a H-burning shell at the bottom of the accreted layer on the WD, a shock wave may appear and/or a strong radiation driven wind develops (e.g., Webbink et al. 1987; Gallagher & Starrfield 1978; Starrfield 1989; Shara 1989; Starrfield et al. 1990; Kato & Hachisu 1994). Calculations show that not all the accreted material is ejected, but a substantial fraction (10–90%, depending on the system parameters) can remain on the WD (e.g., Starrfield et al. 1972). Residual H burning of the remaining material in a shell on the WD can thus take place which gives rise to radiation at a constant luminosity, $L_{\rm Edd}$ (referred to as the 'constant bolometric luminosity', CBL, phase). If not all of the accreted material is burned and blown away, the WD mass may increase towards the Chandrasekhar mass after a large number of outbursts in RNe, eventually leading to a type Ia supernova event or to the formation of a neutron star by accretion induced

collapse (e.g., Della-Valle & Livio 1996; Orio & Greiner 1999; but see González-Riestra et al. 1998).

A short-lived X-ray emission phase ($\lesssim$1 day) is predicted when the energy of the burning shell first reaches the surface of the WD (Starrfield et al. 1990). The energy is then put into the envelope, which leads to a rapid expansion of the WD photosphere up to $\sim 100\,R_\odot$; this leads to a drop in $T_{\rm eff}$. As the WD photosphere subsequently shrinks back through the ejected material to the equilibrium radius of the WD during the CBL phase, $T_{\rm eff}$ of the photosphere increases again and the peak of the emitted spectrum shifts from visual to UV and finally to the X-ray band (Ögelman et al. 1987, 1993; Shore et al. 1994; MacDonald 1996; Balman et al. 1998, and references therein). At this stage the object is expected to radiate at $L_{\rm X}\sim 10^{38}\,{\rm erg\,s^{-1}}$ with $kT_{\rm eff}\sim$20–85 eV (e.g., Starrfield 1979; Prialnik 1986), very much like a SSS (see §11). The duration of the CBL phase is expected to last a few years or less, and is proportional to the left-over envelope mass, which in turn is predicted to be inversely proportional to $M_{\rm WD}$ (e.g., Prialnik 1986; Starrfield 1989; Kato & Hachisu 1989, 1994; Kato 1997; see also González-Riestra et al. 1998, and references therein). Some novae do not show X-rays during the early stages of outburst. This may be attributed to a large column density of the ejecta and argues in favour of high masses for the expelled gas (e.g., Shore et al. 1996). Note that during the first part of the CBL phase the *observed* soft X-ray flux may still increase, due to the clearing of the ejected material as it expands and its density decreases (Krautter et al. 1996). Once the H burning ceases, the WD photosphere is expected to cool at a constant radius, and $L_{\rm X}$ drops gradually. Finally, when novae return to quiescence, accretion may resume again, and they then appear as an ordinary CV. The total energy emitted during all stages is $\sim 10^{44}$–10^{46} erg.

In addition to the soft component due to H-burning, shocks in the hot circumstellar material can produce hard X-ray emission* (e.g., Brecher et al. 1977; Willson et al. 1984; Ögelman et al. 1987; O'Brien et al. 1994; Balman et al. 1998, and references therein). Even if there is no shock wave in the outburst, shocks may originate in interacting winds, or they may be due to interaction between ejecta and pre-existing material. E.g., in RNe and SBNe the donor is a giant star (often a Mira-type object in SBNe; see also §10.7), which has lost a significant amount of material through a wind. Note that CNe typically have main-sequence dwarf donors, which will not have significant stellar winds. Alternatively, shocks may occur in the ejected shells during the different phases of the nova outburst. The expected hard X-ray spectrum is thermal, with $kT_{\rm eff}\sim$0.2–15 keV, depending on how much time has elapsed since the shock, and how efficient the cooling is, and with $L_{\rm X}\simeq 10^{33}$–$10^{34}\,{\rm erg\,s^{-1}}$ (e.g., Lloyd et al. 1992; O'Brien et al. 1994). Additionally a collection of emission lines are expected. Compton scattering of γ-rays produced in the decay of ^{22}Na and ^{26}Al to X-ray energies are expected to also give rise to hard X-ray emission (Starrfield et al. 1992; Livio et al. 1992; Pistinner et al. 1994). However, this may only become important at $kT\gtrsim 6$ keV (Livio et al. 1992); moreover, they are probably not the main source of hard X-rays (Starrfield et al. 1992).

* Although we here refer to emission typically $\gtrsim$0.1 keV, we call it *hard* X-ray emission in order to distinguish it from the soft component due to H-burning.

10.6.2 Super-soft X-ray emission

The CN GQ Mus (Nova Mus 1983) was the first nova to show supersoft emission similar to SSS (Ögelman et al. 1993; §11). Subsequently, more novae were found to exhibit such a phase, i.e., the CNe V1974 Cyg (Nova Cyg 1992; Krautter et al. 1996; Balman et al. 1998), Nova LMC 1995 (Orio & Greiner 1999), V2487 Oph (Nova Oph 1998; Hernanz & Sala 2002), V382 Vel (Nova Vel 1999; Orio et al. 2002), and V1494 Aql (Nova Aql 1999 No. 2; e.g., Starrfield et al. 2001), and the RN U Sco (Kahabka et al. 1999). The soft component has best-fit temperatures of $kT \simeq 30$–$80\,\mathrm{eV}$ with $L_\mathrm{X} \sim 10^{37}$–$10^{38}\,\mathrm{erg\,s^{-1}}$. About 20% of the observed novae have shown a supersoft phase (although not all novae have been followed closely enough to exclude such a phase). One of the reasons put forward why not all novae show a supersoft phase is that in most novae all the H might be depleted soon after the outburst, therefore providing no time for a CBL phase (Orio et al. 2001a). Simple X-ray fits such as a black-body do not describe the soft component well (see, e.g., Kahabka et al. 1999; Balman & Krautter 2001; Orio et al. 2002). This is because the spectral energy distribution of a hot WD differs considerably from a black-body (e.g., MacDonald & Vennes 1991; Jordan et al. 1994; Hartmann & Heise 1997).

The X-ray turn-off times for CNe are generally <3–7 years (e.g., Szkody & Hoard 1994; Orio et al. 1996; Hernanz & Sala 2002; see also González-Riestra et al. 1998), suggesting that most of the CNe run out of nuclear fuel in the course of a few years after outburst. V1974 Cyg (see §10.6.4) turned off only ∼18 months after outburst (Krautter et al. 1996). The turn-off times are much shorter than the nuclear burning times, and imply that the WD has ejected most of its envelope during or soon after the outburst. Note that GQ Mus turned off ∼9–10 years after outburst (Shanley et al. 1995); at that time the temperature of the cooling remnant was ∼10 eV. This is somewhat longer than most novae, and it is argued that either more mass was left on the WD than generally inferred, or that the short P_orb, 85.5 min, of GQ Mus and the small donor mass had enhanced the effects of irradiation of the donor (e.g., Diaz & Steiner 1994). This in turn may have induced continued accretion on the WD and prolonged the CBL phase (Ögelman et al. 1993; Shanley et al. 1995).

The RN CI Aql showed faint ($\sim 10^{33}\,\mathrm{erg\,s^{-1}}$) and very soft ($kT \sim 40$–$50\,\mathrm{eV}$) X-ray emission, 14 and 16 months after the outburst. However, this is not due to H-burning; that phase had already ceased before that time. The observed X-ray emission is suggested to be either due to ionisation of the circumstellar material or due to shocks within the wind and/or with the surrounding medium (Greiner & Di Stefano 2002).

In SBNe most of the accreted mass onto the WD is burned quietly for decades, instead of being ejected away quickly as in most CNe. Two SBNe showed supersoft X-ray spectra and luminosities (RR Tel: Jordan et al. 1994; Mürset & Nussbaumer 1994; SMC3/RX J0048.4−7332: Kahabka et al. 1994; Jordan et al. 1996).

10.6.3 Hard X-ray emission

Hard X-ray emission attributed to shocked gas was first detected from the SBN RS Oph in its 1985 outburst. The shocked gas is due to the expanding nova shell colliding with the red-giant wind (e.g., Bode & Kahn 1985). Most CNe and RNe emit hard X-rays in the first months of the outburst with L_X peaking at $\sim 10^{33}$–$10^{34}\,\mathrm{erg\,s^{-1}}$ and bremsstrahlung temperatures in the range 0.5–20 keV (e.g., Orio et al. 2001a,

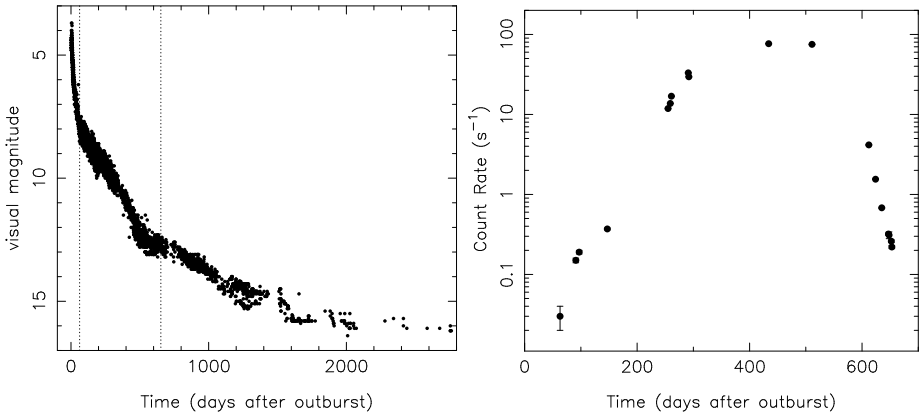

Fig. 10.8. Optical light curve (*left*) based on visual and V-band measurements reported to the VSOLJ (Variable Star Observers League in Japan), VSNET (Variable Star NETwork) and AFOEV (Association Française des Observateurs d'Étoiles Variables), and X-ray light curve (*right*; from Krautter et al. 1996) based on *ROSAT*/PSPC data (0.1–2.4 keV) of the CN V1974 Cyg (Nova Cyg 1992). The start of the outburst is at Feb 19, 1992. In the left panel we indicate with dotted lines the time span of the right panel.

and references therein). The eclipsing, fast ($t_3 \simeq 3$ days*) CN V838 Her (Nova Her 1991) was detected in hard X-rays 5 days after the outburst, with a $kT \sim 10$ keV bremsstrahlung spectrum (Lloyd et al. 1992). The hard emission generally lasts for at least $\simeq 2$ years and even much longer under special circumstances like pre-existing circumstellar material, or a prolonged wind phase (e.g., Orio et al. 2001a).

SBNe show generally hard X-ray emission with $L_X \lesssim 10^{30}$–3×10^{33} erg s^{-1}. When plotted as time since outburst, there seems to be a general decay law for the X-ray flux in SBNe following outburst (Allen 1981; Kwok & Leahy 1984; Hoard et al. 1996; Mürset et al. 1997). This is consistent with the decay times of SBNe after the outburst of the order of decades.

10.6.4 V1974 Cyg and V382 Vel

Two CNe, V1974 Cyg and V382 Vel, have been monitored quite frequently in X-rays during the decline from their outburst.

V1974 Cyg was optically a bright nova (Fig. 10.8). It was the first nova to be observed at all wavelengths from γ-rays to radio. It was a moderately fast nova ($t_3 \sim 35$ days) and it was followed from the early rise of the X-ray flux through the time of maximum to the turnoff (Krautter et al. 1996; Fig. 10.8). The initial observations showed a hard component with a peak around 1 keV. Subsequently, during the X-ray rise, a much softer component appeared that dominated the spectrum at maximum. This soft component decayed more rapidly (by a factor of ~ 35) than the hard component. During the early rise N_H decreased and then leveled off. The rise in the soft component flux and the decrease in N_H is consistent with the clearance of the nova ejecta. The X-ray spectra were best fitted by a WD atmosphere emission model (soft component; $\lesssim 1$ keV) and a Raymond-Smith model of thermal plasma

* t_3 is the time it takes for the nova to decrease by 3 visual magnitudes.

(hard component; $\gtrsim$1 keV), see Balman et al. (1998). The duration of the CBL is inferred to be $\gtrsim$511 days (Krautter et al. 1996).

The hard component spectrum evolved independently of the soft component. The maximum of the hard X-ray emission was reached $\sim$150 days after the outburst with $L_{\rm X}\sim 0.8$–$2\times10^{34}\,{\rm erg\,s^{-1}}$. The time evolution of the hard X-ray flux and the fact that the plasma temperatures decreased from 10 keV to 1 keV suggest emission from shock-heated gas (Balman et al. 1998). This component arose from the interaction of the expanding nova wind with density inhomogeneities, as is also indicated by *Hubble Space Telescope* images within the shell (Paresce et al. 1995).

UV observations showed that $\sim$500 days after the outburst the ejecta reached maximum ionisation and then started to recombine (Shore et al. 1996). This is coincident with the start of the X-ray turn off observed in X-rays. The decrease in the ionisation fraction of the ejecta can be interpreted as a change in the photo-ionisation rate from the central source and is due to a decrease in luminosity and $T_{\rm eff}$ after the cessation of nuclear burning. Two years after the X-ray turn-off a $kT_{\rm eff}\simeq$2 eV (20 000 K) for the WD was inferred (Shore et al. 1997). It is possible that the initial X-ray decline in V1974 Cyg was the result of a cooling WD in which most of the energy was radiated outside the X-ray band pass, rather than representing a return to final quiescence. This implies a longer cooling time, hence a larger amount of mass remaining on the WD (Shore et al. 1997).

V382 Vel was a relatively fast nova ($t_3\sim$10 days). A short *RXTE* observation was performed $\sim$3 days after the peak of the optical outburst, but no X-rays were seen. Hard X-rays were detected $\sim$15–17 days after the peak of the optical outburst with $kT\sim$6–10 keV (Orio et al. 2001b; Mukai & Ishida 2001). In the first two months after the outburst it cooled rapidly to $kT\simeq$2.4 keV (Mukai & Ishida 2001). $L_{\rm X}$ was $\sim5\times10^{34}\,{\rm erg\,s^{-1}}$ for about 3–5 weeks. As the initially strong intrinsic absorption ($N_{\rm H}\sim2\times10^{23}\,{\rm cm^{-2}}$; Orio et al. 2001b) of the ejected nebula was thinning out, the equivalent $N_{\rm H}$ decreased to $\sim2\times10^{22}\,{\rm cm^{-2}}$ (Mukai & Ishida 2001). Four months later the hard component had cooled to a plasma temperature of $kT<$1 keV and the absorption column was close to the interstellar value of $N_{\rm H}\sim10^{21}\,{\rm cm^{-2}}$ (Orio et al. 2001b). The hard X-ray emission is interpreted as the result of a shock internal to the nova ejecta. The initial ejecta provide the absorbing column; a layer of later and faster moving ejecta plough into the initial ejecta. Note that in the first X-ray observations a weak Fe K line at $\simeq$6.6 keV, with EW$\sim$130 eV, was seen. The weakness of the Fe K line is consistent with the shock model, provided that the shocked plasma is not in ionisation equilibrium (Mukai & Ishida 2001).

About six months after the outburst peak V382 Vel appeared as a bright SSS (Orio et al. 2002). The supersoft X-rays were variable by a factor of $\sim$2 on a time scale of minutes. The hard component did not show such variability. Note that variability was also seen in soft X-rays from V1494 Aql, about 10 months after the outburst: it showed a flare which lasted for $\sim$15 min; additionally a periodicity near 42 min was found (Drake et al. 2003).

Four months later, the continuum emission from V382 Vel was gone; instead an emission line spectrum, from highly ionised ions, in the supersoft range was inferred. These emission lines presumably have their origin in ionisation within the ejected nebula. Note that some of the spectra taken with relatively low resolution may

appear softer if there is a strong superimposed nebular emission. The WD then appears to be cooler than obtained from the spectral fits (Orio et al. 2002).

V382 Vel was followed for a further period of 8 months, starting 7 months after the outburst. Within a period of less than 6 weeks the flux had dropped by a factor ∼200. Thereafter this component continued to decline more slowly, but still somewhat faster than the hard X-rays. The spectra during this period show a wealth of emission lines, which mainly come from H and He-like transitions of Mg, Ne, O, N and C, as well as some Si and Na lines. Most of the lines are broadened with FWHM∼2000 km s^{-1}, which is compatible with the velocity of the expanding shell. The He-like triplets of O VII and N VI constrain the plasma temperature to $kT \simeq 39$–43 eV (Burwitz et al. 2002b). One possibility is that during the late phase of the nova, when the shell has become transparent, the medium around the system is ionised by the still UV/EUV bright WD. Alternatively, the line dominated spectrum could result from the interaction of the expanding shell with the circumstellar material, shocks within the expanding shell, or from shocks due to collisions of a fast wind with the interstellar matter (Greiner & Di Stefano 2002).

10.6.5 Quiescent, old novae

Novae in quiescence are often referred to as 'old' novae. Sample studies of old novae show X-ray emission with typically $L_{\rm X} \simeq 10^{30}$–10^{33} erg s^{-1} and $kT \gtrsim 1$ keV, when detected (e.g., Becker 1981, 1989; Becker & Marshall 1981; Córdova & Mason 1983; Orio et al. 1993, 2001; Balman et al. 1995; Ögelman & Orio 1995). This is comparable to that found for quiescent DNe (see §10.2.1), although the optical quiescent novae are at least ∼10 times brighter. Fast novae appear to be brighter than slow novae in quiescence (Becker & Marshall 1981; Orio et al. 2001a). Note that V2487 Oph is the first nova to be detected in quiescence both before and after the outburst, with similar fluxes (Hernanz & Sala 2002). The mass transfer rates derived from $L_{\rm X}$ are much lower than those inferred from other wavelengths, similar to that found for DNe (see §§10.2.3, 10.2.4). In this case it might be that the BL radiation is emitted entirely in the EUV. The ratio of $L_{\rm X}$ (0.2–2.4 keV) to $L_{\rm opt}$ varies from 0.005 (DQ Her/Nova Her 1934) to 4.8 (e.g., CP Pup/Nova Pup 1942); for the majority of the systems the value is less than 0.01 (Orio et al. 2001a).

GK Per (Nova Per 1901) is the first nova for which a CN shell was detected in X-rays (Balman & Ögelman 1999; Balman 2002). The X-ray nebula is asymmetric and composed of knots/clumps. The temperature and ionisation structures do not vary much across the nebula. Its X-ray spectrum is thermal with at least two temperature components, i.e., $kT \sim 0.2$ keV with $L_{\rm X} \sim 2 \times 10^{31}$ erg s^{-1} and $kT > 30$ keV with $L_{\rm X} \sim 3 \times 10^{31}$ erg s^{-1}. Distinct Ne IX emission is seen. The knots/clumps are thought to be the result of fragmentation and condensation in the post-shock material. The existence of the X-ray shell in contrast to other CNe is attributed to the high ambient density.

An outlier among the old novae is T Pyx. This RN showed 5 outbursts between 1890 and 1966. Its outbursts are like those of slow novae, whereas all other RNe show fast nova outbursts. Its luminosity in quiescence is higher than other quiescent novae, $L_{\rm X} \simeq 1$–3×10^{36} erg s^{-1}. This has been attributed to steady nuclear burning on the WD (e.g., Webbink et al. 1987).

10.7 X-ray emission from symbiotic binaries

SBs (e.g., Kenyon 1986) are divided into two subcategories based on their IR colours. S-type ('stellar') systems have IR colours like those if isolated field red giants, whereas D-type ('dusty') systems have IR colours which are redder, indicative of dust. D-type systems generally contain Mira variables with very high mass-loss rates. The wind is ionised by the WD giving rise to the symbiotic nebula.

SBs show small 'outbursts' where the optical increases by ∼1–2 mag on time scales of years. The origin of these outbursts is still rather unclear. They may be related to quasi-steady burning of matter on the WD, shell flashes, or unstable accretion. Symbiotic Novae (SBNe) are a small subgroup of the SBs. They undergo large amplitude (∼7 mag increase) outbursts with durations on the order of decades. These outbursts are thought to be due to thermonuclear runaway events on the surface of the WD. SBNe are discussed in §10.6.

Many of the SBs are detected in X-rays. The most X-ray luminous are the D-types, whereas the S-types are typically two orders of magnitude fainter. Also, SBNe are generally brighter in X-rays compared to the other SBs. This is probably because the average luminosities of SBNe are higher than for the other SBs. SBs have been shown to emit either supersoft X-ray emission, and/or hard X-ray emission from an optically thin plasma with $kT \sim 0.25$–$1.3\,\mathrm{keV}$ with $L_\mathrm{X} \sim 10^{30}$–$10^{33}\,\mathrm{erg\,s^{-1}}$, or even harder X-ray emission, as from an accreting neutron star (see, e.g., Mürset et al. 1997, and references therein).

The hard X-ray emission may be due to the colliding winds of the red giant and the WD (e.g., Willson et al. 1984; Kwok & Leahy 1984), jets (Kellogg et al. 2001; see also Viotti et al. 1987; Leahy & Volk 1995), jets colliding with interstellar material (e.g., Viotti et al. 1987; Ezuka et al. 1998), X-ray emission from the red giant (see, e.g., Ezuka et al. 1998), or accretion onto the WD (e.g., Leahy & Taylor 1987; Jordan et al. 1994). The hard X-ray spectrum of CH Cyg was interpreted as being composed of two components (e.g., Leahy & Volk 1995; Ezuka et al. 1998). However, Wheatley (2001) showed that this emission may be solely due to radiation from the WD which is strongly absorbed by a partionally ionised wind from the red giant.

In SBs, Bondi-Hoyle capture of the red giant wind gives $\dot{M} \sim 10^{-8}\,\mathrm{yr^{-1}}$ onto the WD, which could produce nuclear burning in some systems (e.g., Sion & Starrfield 1994). This might give rise to supersoft X-ray emission, similar to that seen in CNe and RNe (see §10.6) and other SSS (see §11). Depending on how much matter the WD receives and steadily burns, it may be able increase its mass. SBs have therefore been also put forward as candidates for Type Ia supernovae (e.g., Munari & Renzini 1992). It has been noted, however, that either not enough mass can be accreted from the donor, or a mass outflow from the WD may inhibit such a phase (Mürset & Nussbaumer 1994; Mürset et al. 1997).

SBs have indeed shown supersoft X-ray emission (e.g., Mürset et al. 1997; see also §10.6.2). For example, X-ray spectra during quiescence of AG Dra, which is one of the brightest X-ray sources among the SBs (e.g., Anderson et al. 1981), showed a soft component with a temperature of $kT_\mathrm{bb} \simeq 14$–$15\,\mathrm{eV}$ (Greiner et al. 1997; see also Piro et al. 1985; Kenyon 1988). The X-ray luminosity remained constant during quiescence at a level of $L_\mathrm{X} \simeq 10^{37}\,\mathrm{erg\,s^{-1}}$ (Greiner et al. 1997).

AG Dra was the first SB to be observed during outburst in X-rays (Viotti et al.

1995). During the minor (ΔV$\sim$1 mag) and major (ΔV$\sim$2 mag) outbursts it displays different behaviour. During both outbursts the X-ray flux drops, however, kT decreased by a few eV during major outbursts, while it increases by a few eV during minor outbursts. The behaviour during major outbursts is explained by expansion (factor 2–6) and cooling of the WD atmosphere, which also explains the anti-correlation between optical/UV and X-ray fluxes (Greiner et al. 1997; González-Riestra et al. 1999). The cooling could be the result of an increased $\dot{M}$ onto the compact object causing it to expand slowly (Greiner et al. 1997). The drop in X-ray flux during minor outbursts might be attributed to the increased absorbing layer between the X-ray source and observer (Friedjung 1988). During a minor outburst Z And radiated also well above $\sim$1 keV, possibly due to the red-giant wind colliding with material ejected during the outburst (Sokoloski et al. 2002).

10.8 Concluding remarks

During the last decade there has been a staggering flow of new information, not only in X-rays, but also from other wavelengths. Nowadays, substantial progress in understanding the behaviour of CVs is generally made through multi-wavelength efforts. Unfortunately, the space available in this chapter has not allowed us to fully discuss observations across the whole electro-magnetic spectrum. Nevertheless, we have shown that our somewhat 'restricted' view at EUV and X-ray wavelengths has revealed a great variety of rich phenomena taking place in the environment of an accreting WD.

Substantial improvements in our understanding of CVs at high energies are already coming from the instruments on board *Chandra* and *XMM-Newton* and further advances are inevitable over the next few years. These instruments provide the necessary spectral resolution to perform sensible temperature and velocity diagnostics from individually resolved lines and line ratios; something we have previously been used to at optical wavelengths. These exquisite instruments and those which are yet to come will provide us with much more insight into the physical processes which give rise to the rich phenomenology of CVs. This applies to all facettes of CV-research addressed in this Chapter, processes of energy release in magnetic and non-magnetic environments, radiation hydrodynamics, dynamical processes in close binaries and the long-term close binary evolution.

Acknowledgements

We acknowledge discussions with K. Beuermann, J.-P. Lasota, C. Mauche, M. Orio, J. Sokoloski, S. Starrfield and P. Wheatley. AS is supported by the German Bundesministerium für Bildung und Forschung through the Deutsches Zentrum für Luft- und Raumfahrt e.V. (DLR) under grant number 50 OR 9706 8. BW is supported by research funds from the University of Cape Town.

References

Allan, A., Hellier, C., Beardmore, A. (1998), MNRAS 295, 167
Allan, A., et al. (1996), MNRAS 279, 1345
Allen, D.A. (1981), MNRAS 197, 739
Anderson, C.M., Cassinelli, J.P., Sanders, W.T. (1981), ApJ 247, L127
Armitage, P.J., Livio, M. (1996), ApJ 470, 1024

Armitage, P.J., Livio, M. (1998), ApJ 493, 898
Aizu, K. (1973), Prog. Theor. Phys. 49, 1184
Bailey, J. (1995), ASP Conf. Ser. 85, p. 10
Balman, S. (2002), ASP Conf. Ser. 261, p. 617
Balman, S., Krautter, J. (2001), MNRAS 326, 1441
Balman, S., Ögelman, H.B. (1999), ApJ 518, L111
Balman, S., Orio, M., Ögelman, H. (1995), ApJ 449, L47
Balman, S., Krautter, J., Ögelman, H. (1998), ApJ 499, 395
Baskill, D.S., Wheatley, P.J., Osborne, J.P. (2001), MNRAS 328, 71
Bath, G.T., Evans, W.D. & Pringle, J.E. (1974a), MNRAS 166, 113
Bath, G.T., et al. (1974b), MNRAS 169, 447
Beardmore, A.P., Osborne, J.P., Hellier, C. (2000), MNRAS 315, 307
Beardmore, A.P., et al. (1998), MNRAS 297, 337
Becker, R.H. (1981), ApJ 251, 626
Becker, R.H. (1989), in Classical Novae, eds. M.F. Bode & A. Evans, Wiley, New York, p. 215
Becker, R.H., Marshall, F.E. (1981), ApJ 244, L93
Belloni, T., Psaltis, D., van der Klis, M. (2002), ApJ 572, 392
Belloni, T., et al. (1991), A&A 246, L44
Beuermann, K. (1999), MPE Report 272, p. 410
Beuermann, K., Burwitz, V. (1995), ASP Conf. Ser. 85, p. 99
Beuermann, K., Schwope A. (1994), ASP Conf. Ser. 56, p. 119
Beuermann, K., Thomas, H.-C. (1993), AdSpR 13, 115
Beuermann, K., Thomas, H.-C., Pietsch, W. (1991), A&A 246, L36
Bode, M.F., Kahn, F.D. (1985), MNRAS 217, 205
Bonnet-Bidaud, J.M., Mouchet, M. (1987), A&A 188, 89
Brecher, K., Ingham, W.H., Morrison, P. (1977), ApJ 213, 492
Buckley, D.A.H., Tuohy, I.R. (1989), ApJ 344, 376
Buckley, D.A.H., et al. (1997), MNRAS 287, 117
Burwitz, V., et al. (1996), A&A 310, 25
Burwitz, V., et al. (2002a), ASP Conf. Ser. 261, p. 137
Burwitz, V., et al. (2002b), AIP Conf. Proc. 637, p. 377
Córdova, F.A., 1995, in X-ray Binaries, eds. W.H.G. Lewin, et al., CUP, p. 331
Córdova, F.A., Mason, K.O. (1983), in Accretion driven Stellar X-ray sources, eds. W.H.G. Lewin & E.P.J. van den Heuvel, CUP, p. 147
Córdova, F.A., Mason, K.O. (1984), MNRAS 206, 879
Córdova, F.A., Mason, K.O., Nelson, J.E. (1981), ApJ 245, 609
Córdova, F.A., et al. (1980a), MNRAS 190, 87
Córdova, F.A., et al. (1980b), ApJ 235, 163
Córdova, F.A., et al. (1984), ApJ 278, 739
Cropper, M. (1990), SSRv 54, 195
Cropper, M., Ramsay G., Wu., K. (1998), MNRAS 293, 222
Cropper, M., Wu, K., Ramsay G. (2000), NewAR 44, 57
de Martino, D., et al. (2001), A&A 377, 499
Della-Valle, M., Livio, M. (1996), ApJ 473, 240
Diaz, M.P., Steiner, J.E. (1994), ApJ 425, 252
Done C., Magdziarz, P. (1998), MNRAS 298, 737
Done, C., Osborne, J.P. (1997), MNRAS 288, 649
Drake, J.J., et al. (2003), ApJ 584, 448
Drew, J., Verbunt, F. (1985), MNRAS 213, 191
Duck, S.R., et al. (1994) MNRAS 271, 372
Eracleous, M., Halpern, J., Patterson, J. (1991a), ApJ 382, 290
Eracleous, M., Patterson, J., Halpern, J. (1991b), ApJ 370, 330
Ezuka, H., Ishida, M., Makino, F. (1998), ApJ 499, 388
Ferland, G.J., et al. (1982), ApJ 262, L53
Fischer A., Beuermann K. (2001), A&A 373, 211
Fontaine, G., Montmerle, T., Michaud, G. (1982), ApJ 257, 695
Frank, J., King, A.R., Lasota, J.-P. (1987), A&A 178, 137

Frank, J., King, A.R., Lasota, J.-P. (1988), A&A 193, 113
Frank, J., King, A.R., Raine, D. (1992), Accretion Power in Astrophysics, 2nd edition, CUP
Friedjung, M. (1988), Proc. IAU Coll. 103, p. 199
Fujimoto, R., Ishida, M. (1995), ASP Conf. Ser. 85, p. 136
Gallagher, J.S., Starrfield, S. (1978), ARA&A 16, 171
Gänsicke, B.T., Beuermann, K., de Martino, D. (1995), A&A 303, 127
González-Riestra, R., Orio, M., Gallagher, J. (1998), A&ASS 129, 23
González-Riestra, R., et al. (1999), A&A 347, 478
Greiner, J. (1999), A&A 336, 626
Greiner, J., Di Stefano, R. (2002), ApJ 578, L59
Greiner, J., van Teeseling, A. (1998), A&A 339, L21
Greiner, J., et al. (1997), A&A 322, 576
Greiner, J., et al. (1999), A&A 343, 183
Haberl, F., Motch, C. (1995), A&A 297, L37
Haberl, F., et al. (1994), A&A 291, 171
Hack, M., La Dous, C. (1993), Cataclysmic Variables and Related Objects, NASA SP-507
Haefner, R, Schoembs, R., Vogt, N. (1979), A&A 77, 7
Hameury, J.-M., King, A.R., Lasota, J.-P. (1986), MNRAS 218, 695
Hartmann, H.W., Heise, J. (1997), A&A 322, 591
Hartmann, H.W., et al. (1999), A&A 349, 588
Heise, J., et al. (1985), A&A 148, L14
Heise, J., et al. (1978), A&A 63, L1
Hellier, C. (1991), MNRAS 251, 693
Hellier, C. (1992), MNRAS 258, 578
Hellier, C. (1996), Proc. IAU Coll. 158, p. 143
Hellier, C. (1997), MNRAS 291, 71
Hellier, C., Beardmore, A.P. (2002), MNRAS 331, 407
Hellier, C., Cropper, M., Mason, K.O. (1991), MNRAS 248, 233
Hellier, C., Garlick, M.A., Mason, K.O. (1993), MNRAS 260, 299
Hellier, C., Mukai, K., Beardmore, A.P. (1997), MNRAS 292, 397
Hellier, C., Mukai, K., Osborne, J.P. (1998), MNRAS 297, 526
Hellier, C., et al. (1989), MNRAS 238, 1107
Hellier, C., et al. (1996), MNRAS 280, 877
Hempelmann, A., et al. (1995), A&A 294, 515
Hernanz, M., Sala, G. (2002), Science 298, 393
Hessman, F.V., Gänsicke, B.T., Mattei, J.A. (2000), A&A 361, 952
Hoare, M.G., Drew, J.E. (1991), MNRAS 249, 452
Hoard, D.W., Wallerstein, G., Willson, L.A. (1996), PASP 108, 81
Horne, K., et al. (1994), ApJ 426, 294
Iben, Jr. I., Livio, M. (1993), PASP 105, 1373
Ishida, M. (1991), PhD thesis, University of Tokyo
Ishida, M., Ezuka, H. (1999), ASP Conf. Ser. 157, p. 333
Ishida, M., Fujimoto, R. (1995), ASP Conf. Ser. 85, p. 132
Ishida, M., et al. (1992), MNRAS 254, 647
Jensen, K.A. (1984), ApJ 278, 278
Jones, M.H., Watson, M.G. (1992), MNRAS 257, 633
Jordan, S., Mürset, U., Werner, K. (1994), A&A 283, 475
Jordan, S., et al. (1996), A&A 312, 897
Kahabka, P., Pietsch, W., Hasinger, G. (1994), A&A 288, 538
Kahabka, P., et al. (1999), A&A 347, L43
Kallman, T.R., Jensen, K.A. (1985), ApJ 299, 277
Kamata, Y., Koyama K. (1993), ApJ 405, 307
Kato, M. (1997), ApJS 113, 121
Kato, M., Hachisu, I. (1989), ApJ 346, 424
Kato, M., Hachisu, I. (1994), ApJ 437, 802
Katz, J.I. (1975), ApJ 200, 298
Kellogg, E., Pedelty, J.A., Lyon, L.G. (2001), ApJ 563, L151

Kenyon, S.J. (1986), The Symbiotic Stars, CUP
Kenyon, S.J. (1988), Proc. IAU Coll. 103, p. 11
King, A.R. (1997), MNRAS 288, L16
King, A.R., Cannizzo, J.K. (1998), ApJ 499, 348
King, A.R., Lasota, J.-P. (1979) MNRAS 188, 653
King, A.R., Lasota, J.-P. (1991) ApJ 378, 674
King, A.R., Shaviv, G. (1984), MNRAS 211, 883
Knigge, C., et al. (2002), ApJ 580, L151
Krautter, J. (2002), AIP Conf. Proc. 637, p. 345
Krautter, J., et al. (1996), ApJ 456, 788
Krzemiński, W., Serkowski, K. (1977), ApJ 216, L45
Kuijpers, J., Pringle, J.E. (1982), A&A 114, L4
Kunze, S., Speith, R., Hessman, F.V. (2001), MNRAS 322, 499
Kuulkers, E., et al. (1998), ApJ 494, 753
Kuulkers, E., et al. (2002), ASP Conf. Proc. 261, p. 443
Kwok, S., Leahy, D.A. (1984), ApJ 283, 675
Lamb, D.Q., Masters, A.R. (1979), ApJ 234, L117
Lasota, J.-P. (2001), NewAR 45, 449
Lasota, J.P., Hameury, J.M., Huré, J.M. (1995), A&A 302, L29
Leahy, D.A., Taylor, A.R. (1987), A&A 176, 262
Leahy, D.A., Volk, K. (1995), ApJ 440, 847
Litchfield, S.J., King, A.R. (1990), MNRAS 247, 200
Livio, M., Pringle, J.E. (1992), MNRAS 259, 23P
Livio, M., et al. (1992), ApJ 394, 217
Lloyd, H.M., et al. (1992), Nat 356, 222
Long, K.S., et al. (1996), ApJ 469, 841
Lynden-Bell, D., Pringle, J.E. (1974), MNRAS 168, 603
MacDonald, J. (1996), Proc. IAU Coll. 158, p. 281
MacDonald, J., Vennes, S. (1991), ApJ 371, 719
Marsh, T.R. (1999), MNRAS 304, 443
Marsh, T.R., Steeghs, D. (2002), MNRAS 331, L7
Mason, K.O. (1985), SSRv 40, 99
Mason, K.O. (1986), Lecture Notes in Physics 266, p. 29
Mason, K.O., Drew, J.E., Knigge, C. (1997), MNRAS 290, L23
Mason, K.O., et al. (1978), ApJ 226, L129
Mason, K.O., et al. (1988), MNRAS 232, 779
Mason, K.O., et al. (1992), MNRAS 258, 749
Matt, G., et al. (2000), A&A 358, 177
Mauche, C.W. (1996a), ApJ 463, L87
Mauche, C.W. (1996b), Proc. IAU Coll. 158, p. 243
Mauche, C.W. (1997), ApJ 476, L85
Mauche, C.W. (1999), ASP Conf. Ser. 157, p. 157
Mauche, C.W. (2002a), ApJ 580, 423
Mauche, C.W. (2002b), ASP Conf. Ser. 261, p. 113
Mauche, C.W., Mukai, K. (2002), ApJ 566, L33
Mauche, C.W., Raymond, J.C. (1987), ApJ 323, 690
Mauche, C.W., Raymond, J.C. (2000), ApJ 541, 924
Mauche, C.W., Robinson, E.L. (2001), ApJ 562, 508
Mauche, C.W., Liedahl, D.A., Fournier, K.B. (2001), ApJ 560, 992
Mauche, C.W., Raymond, J.C., Mattei, J.A. (1995), ApJ 446, 842
Mauche, C.W., et al. (1991), ApJ 372, 659
Meyer, F., Meyer-Hofmeister, E. (1994), A&A 288, 175
Motch, C., et al. (1996), A&A 307, 459
Mukai, K. (1995), ASP Conf. Ser. 85, p. 119
Mukai, K. (2000), NewAR 44, 9
Mukai, K., Ishida, M. (2001), ApJ 551, 1024
Mukai, K., Shiokawa, K. (1993), ApJ 418, 863

Mukai, K., et al. (1997), ApJ 475, 812
Mukai, K., et al. (2003), ApJ 586, L77
Munari, U., Renzini, A. (1992), ApJ 397, L87
Mürset, U., Nussbaumer, H. (1994), A&A 282, 586
Mürset, U., Wolff, B., Jordan, S. (1997), A&A 319, 201
Narayan, R., Popham, R. (1993), Nat 362, 820
Naylor, T., La Dous, C. (1997), MNRAS 290, 160
Naylor, T., et al. (1987), MNRAS 229, 183
Naylor, T., et al. (1988), MNRAS 231, 237
Norton, A.J. (1993), MNRAS 265, 316
Norton, A.J., Watson, M.G. (1989), MNRAS 237, 853
Norton, A.J., Watson, M.G., King, A.R. (1991), Lecture Notes in Physics 385, p. 155
Norton, A.J., Wynn, G.A., Somerscales, R.V. (2004), ApJ 614, 349
Norton, A.J., et al. (1992a), MNRAS 254, 705
Norton, A.J., et al. (1992b), MNRAS 258, 697
Norton, A.J., et al. (1997), MNRAS 289, 362
Norton, A.J., et al. (1999), A&A 347, 203
O'Brien, T.J., Lloyd, H.M., Bode, M.F. (1994), MNRAS 271, 155
Ögelman, H., Orio, M. (1995), in Cataclysmic Variables, eds. A. Bianchini, et al., Dordrecht, Kluwer, p. 11
Ögelman, H., Krautter, J., Beuermann, K. (1987), A&A 177, 110
Ögelman, H., et al. (1993), Nat 361, 331
Orio, M. (1999), Physics Reports 311, 419
Orio, M., Greiner, J. (1999), A&A 344, L13
Orio, M., Covington, J., Ögelman, H. (2001a), A&A 373, 542
Orio, M., et al. (1993), AdSpR 13, 351
Orio, M., et al. (1996), ApJ 466, 410
Orio, M., et al. (2001b), MNRAS 326, L13
Orio, M., et al. (2002), MNRAS 333, L11
Paczyński, B. (1978), in Nonstationary Evolution in Close Binaries, ed. A. Żytkow, Polish Sci. Publ., Warsaw, p. 89
Paresce, F., et al. (1995), A&A 299, 823
Parmar, A.N., White, N.E. (1988), Mem. Soc. Astr. It. 59, 147
Patterson, J. (1981), ApJS 45, 517
Patterson, J. (1984), ApJS 54, 443
Patterson, J., Price, C. (1980), IAU Circ. 3511
Patterson, J., Raymond, J.C. (1985a), ApJ 292, 535
Patterson, J., Raymond, J.C. (1985b), ApJ 292, 550
Patterson, J., Robinson, E.L., Nather, R.E. (1977), ApJ 214, 144
Patterson, J., Robinson, E.L., Nather, R.E. (1978), ApJ 224, 570
Patterson, J., et al. (1998), PASP 110, 403
Patterson, J., et al. (2001), PASP 113, 72
Piro, L., et al. (1985), IAU Circ. 4082
Pistinner, S., Shaviv, G., Starrfield, S. (1994), ApJ 437, 794
Podsiadlowski, Ph., Han, Z., Rappaport, S. (2003), MNRAS 340, 1214
Polidan, R.S., Holberg, J.B. (1984), Nat 309, 528
Polidan, R.S., Mauche, C.W., Wade, R.A. (1990), ApJ 356, 211
Ponman, T.J., et al. (1995), MNRAS 276, 495
Popham, R., Narayan, R. (1995), ApJ 442, 337
Pratt, G.W., et al. (1999a), MNRAS 307, 413
Pratt, G.W., et al. (1999b), MNRAS 309, 847
Predehl, P., Schmitt, J.H.M.M. (1995), A&A 293, 889
Prialnik, D. (1986), ApJ 310, 222
Pringle, J.E. (1977), MNRAS 178, 195
Pringle, J.E. (1981), ARA&A 19, 137
Pringle, J.E., Rees, M.J. (1972), A&A 21, 1
Pringle, J.E., Savonije, G.J. (1979), MNRAS 187, 777

Pringle, J.E., et al. (1987), MNRAS 225, 73
Psaltis, D., Belloni, T., van der Klis, M. (1999), ApJ 520, 262
Rappaport, S., et al. (1974), ApJ 187, L5
Ramsay, G., et al. (1994,) MNRAS 270, 692
Ramsay, G., et al. (2001a), A&A 365, L288
Ramsay, G., et al. (2001b), A&A 365, L294
Raymond, J.C., Mauche, C.W. (1991), in Extreme Ultraviolet Astronomy, eds. R.F. Malina & S. Bowyer, Pergamon, New York, p. 163
Reimers, D., Hagen, H.-J. (2000), A&A 358, L45
Reimers, D., Hagen, H.-J., Hopp, U. (1999), A&A 343, 157
Richman, H.R. (1996), ApJ 462, 404
Ritter, H., Kolb, U. (2003), A&A 404, 301
Rosen, S.R., Mason, K.O., Córdova, F.A. (1988), MNRAS 231, 549
Rosen, S.R., et al. (1991), MNRAS 249, 417
Rosner, R., Golub, L., Vaiana, G.S. (1985), ARA&A 23, 413
Schlegel, E.M., Singh, J. (1995), MNRAS 276, 1365
Schmitt, J.H.M.M., et al., (1990), ApJ 365, 704
Schwarz, R., et al. (2002), ASP Conf. Ser. 261, p. 167
Schwope, A.D. (1996), Proc. IAU Coll. 158, p. 189
Schwope, A.D. (2001), Lecture Notes in Physics 573, p. 127
Schwope, A.D., et al. (2001), A&A 375, 419
Schwope, A.D., et al. (2002), A&A 392, 541
Shakura, N.I., Sunyaev, R.A. (1973), A&A 24, 337
Shanley, L., et al. (1995), ApJ 438, L95
Shara, M.M. (1989), PASP 101, 5
Shore, S.N., Starrfield, S., Sonneborn, G. (1996), ApJ 463, L21
Shore, S.N., et al. (1994), ApJ 421, 344
Shore, S.N., et al. (1997), ApJ 490, 393
Silber, A., Vrtilek, S.D., Raymond, J.C. (1994), ApJ 425, 829
Sion, E.M., Starrfield, S.G. (1994), ApJ 421, 261
Sion, E.M., et al. (1996), ApJ 471, L41
Sion, E.M., et al. (2002), ASP Conf. Proc. 261, p. 69
Sirk, M.M., Howell, S.B. (1998), ApJ 506, 824
Sokoloski, J.L., et al. (2002), ASP Conf. Proc. 261, p. 667
Starrfield, S. (1979), Proc. IAU Coll. 53, p. 274
Starrfield, S. (1989), in Classical Novae, op. cit., p. 39
Starrfield, S., et al. (1972), ApJ 176, 169
Starrfield, S., et al. (1990), Proc. IAU Coll. 122, p. 306
Starrfield, S., et al. (1992), ApJ 391, L71
Starrfield, S., et al. (2001), Bull. AAS 198, 11.09
Swank, J.H. (1979), Proc. IAU Coll. 53, p. 135
Swank, J.H., et al. (1978), ApJ 226, L133
Szkody, P. (1999), Frontiers Science Ser. 26, p. 53
Szkody, P., Hoard, D.W. (1994), ApJ 429, 857
Szkody, P., Kii, T., Osaki, Y. (1990), AJ 100, 546
Szkody, P., Osborne, J., Hassall, B.J.M. (1988), ApJ 328, 243
Szkody, P., et al. (1996), ApJ 469, 834
Szkody, P., et al. (1999), ApJ 521, 362
Szkody, P., et al. (2002a), ApJ 574, 942
Szkody. P., et al. (2002b), AJ 123, 413
Taylor, P., et al. (1997), MNRAS 289, 349
Tylenda, R. (1981), Acta Astronomica 31, 127
Ulla, A. (1995), A&A 301, 469
van der Woerd, H., Heise, J., Bateson, F. (1986), A&A 156, 252
van der Woerd, H., et al. (1987), A&A 182, 219
van Teeseling, A. (1997a), A&A 319, L25
van Teeseling, A. (1997b), A&A 324, L73

van Teeseling, A., Verbunt, F. (1994), A&A 292, 519
van Teeseling, A., Beuermann, K., Verbunt, F. (1996), A&A 315, 467
van Teeseling, A., Fischer, A., Beuermann, K. (1999), ASP Conf. Ser. 157, p. 309
van Teeseling, A., Verbunt, F., Heise, J. (1993), A&A 270, 159
van Teeseling, A. et al. (1995), A&A 300, 808
Verbunt, F. (1987), A&AS 71, 339
Verbunt, F. (1996), MPE Report 263, p. 93
Verbunt, F., Wheatley, P.J., Mattei, J.A. (1999), A&A 346, 146
Verbunt, F., et al. (1997), A&A 327, 602
Viotti, R., et al. (1987), ApJ 319, L7
Viotti, R., et al. (1995), in Cataclysmic Variables, op. cit., p. 195
Vrtilek, S.D., et al. (1994), ApJ 425, 787
Walker, M.F. (1956), ApJ 123, 68
Warner, B. (1980), IAU Circ. 3511
Warner, B. (1983), Proc. IAU Coll. 72, p. 155
Warner, B. (1986), MNRAS 219, 347
Warner, B. (1995), Cataclysmic Variable Stars, CUP
Warner, B., Robinson, E.L. (1972), Nature Phys. Sci. 239, 2
Warner, B., Woudt, P.A. (2002), MNRAS 335, 84
Warner, B., O'Donoghue, D., Wargau, W. (1989), MNRAS 238, 73
Warner, B., Livio, M., Tout, C.A. (1996), MNRAS 282, 735
Warner, B., Woudt, P.A., Pretorius, M.L. (2003), MNRAS 344, 1193
Warner, B., et al. (1972), MNRAS 159, 321
Warren, J.K., Sirk, M.M., Vallerga, J.V. (1995), ApJ 445, 909
Watson, M.G. (1986), Lecture Notes in Physics 266, p. 97
Watson, M.G., King, A.R., Heise, J. (1985), SSRv 40, 127
Watson, M.G., et al. (1989), MNRAS 237, 299
Webbink, R.F., et al. (1987), ApJ 314, 653
Webbink, R., Wickramasinghe, D.T. (2002), MNRAS 335, 1
Wheatley, P.J. (2001), AIP Conf. Ser. 599, p. 1007
Wheatley, P.J., West, R.G. (2002), ASP Conf. Proc. 261, p. 433
Wheatley, P.J., Mauche, C.W., Mattei, J.A. (2003), MNRAS 345, 49
Wheatley, P.J., et al. (1996a), MNRAS 283, 101
Wheatley, P.J., et al. (1996b), A&A 307, 137
Wheatley, P.J., et al. (2000), NewAR 44, P33
White, N.E., Marshall, F.E. (1980), IAU Circ. 3514
White, N.E., Nagase, F., Parmar, A.N. (1995), in X-ray Binaries, op. cit., p. 1
Wickramasinghe, D.T., Ferrario, L. (2000), PASP 112, 873
Willson, L.A., et al. (1984), A&A 133, 137
Woelk, U., Beuermann, K. (1996), A&A 306, 232
Wood, J.H., Naylor, T., Marsh, T.R. (1995b), MNRAS 274, 31
Wood, J.H., et al. (1995a), MNRAS 273, 772
Woods, A.J., Drew, J.E., Verbunt, F. (1990), MNRAS 245, 323
Woudt, P.A., Warner, B. (2002), MNRAS 333, 411
Wu, K., et al. (2002), MNRAS 331, 221
Wynn, G.A., King, A.R. (1992), MNRAS 255, 83
Yoshida, K., Inoue, H., Osaki, Y. (1992), PASJ 44, 537